2018

IL-17 Drives Copper Uptake and Activation of Growth Pathways in Colorectal Cancer Cells in a Steap4-dependent Manner

Evan Martin
Cleveland State University

IL-17 DRIVES COPPER UPTAKE AND ACTIVATION OF GROWTH PATHWAYS IN COLORECTAL CANCER CELLS IN A STEAP4-DEPENDENT MANNER

EVAN MARTIN

Bachelor of Arts in Chemistry

Case Western Reserve University

May 2014

Submitted in partial fulfillment of requirements for the degree of

MASTER OF SCIENCE IN CHEMISTRY

at the

CLEVELAND STATE UNIVERSITY

December 2018

We hereby approve this thesis for

EVAN MARTIN

Candidate for the Master of Science in Chemistry degree in the

Department of Chemistry

at the CLEVELAND STATE UNIVERSITY'S

College of Graduate Studies by

Thesis Committee Chairperson, Dr. Anthony Berdis

Department & Date

Thesis Committee Chairperson, Dr. Michael Kalafatis

Department & Date

Thesis Committee Chairperson, Dr. Warren Boyd

Department & Date

Student's date of defense: September 11, 2018

ACKNOWLEDGEMENTS

The author would like to gratefully acknowledge Dr. Xiaoxia Li, Dr. Junjie Zhou, Dr. Yun Liao, Dr. Xing Chen, and Dr. James Faulk for their assistance and guidance in this work. Without their hard work, knowledge, dedication, and patience, this project would not have been possible.

IL-17 DRIVES COPPER UPTAKE AND ACTIVATION OF GROWTH PATHWAYS IN COLORECTAL CANCER CELLS IN A STEAP4-DEPENDENT MANNER

EVAN MARTIN

ABSTRACT

Colorectal cancer is a disease characterized by abnormal, invasive cell growth beginning in the colon or rectum. The third most common type of cancer worldwide, approximately one million new cases of the disease are diagnosed across the globe annually, resulting in an estimated 700,000+ deaths. One major risk factor associated with development of colorectal cancer is the presence of chronic inflammation in the large intestine, also known as colitis. Inflammation is a complex immune response against harmful stimuli, characterized by symptoms including heat, redness, swelling and pain. One important molecular mediator of this process is interleukin 17 (IL-17), a pro-inflammatory cytokine. While acute inflammation is a useful defensive response against invading pathogens, the presence of chronic inflammation is associated with an increased risk of tumorigenesis.

Colorectal cancer is frequently observed to metastasize from the colon to the liver, the body's largest storage site of copper, after which it becomes significantly more difficult to treat effectively. Copper is a trace nutrient required by all living systems, due to its ability to participate in one-electron exchange reactions, a vital mechanism of ubiquitous biological processes. STEAP4, a cell membrane protein, is a copper reductase.

In this thesis, data are presented that show that colon cancer cells in which STEAP4 is overexpressed take up more copper from their environment than colon cancer

cells in which STEAP4 is expressed normally. Additional data show that IL-17 stimulation, previously linked to colorectal cancer progression, increases copper uptake by colon cancer cells. A mouse model experiment also shows that induction of colitis mobilizes copper from the liver into systemic circulation. Further, it is shown that overexpression of STEAP4 enhances activation of IL-17-mediated growth pathways that have previously been shown to drive cancer progression. Finally, it is shown that colitis-associated colorectal cancer mice treated with a copper chelator may develop fewer tumor nodules that untreated mice. Taken together, these data suggest that IL-17 signaling drives tumor progression through a STEAP4-dependent mechanism of copper uptake. It is further suggested that lowering body copper levels through chelation therapy could be an effective method of stopping colorectal cancer progression.

TABLE OF CONTENTS

Page

LIST OF TABLES

LIST OF FIGURES

CHAPTER I

GENERAL BACKGROUND

1.1 Copper and Biology

Copper is a transition metal characterized by its malleability and ductility, a reddish-brown color, and high thermal and electrical conductivity. It has a valence electron configuration of $[Ar]3d^{10}4s^1$ and an atomic number of 29 with a standard atomic weight of 63.546. Due to its electron configuration consisting of a fully filled d-shell and a half-filled s-shell, copper may be found naturally in its elemental form, though it can also be found in the form of various ores, such as sulfides, oxides, and carbonates. Copper is also a metal of historical importance to human civilization, as it was the first metal to be smelted from ore, as well as the first metal to be cast as mold and to be alloyed with another metal, tin, to form bronze [1].

Copper is also a critical element to the process of life. An essential element that is necessary for all living systems, including animals, plants, fungi, as well as bacteria, copper plays a role in many different vital functions [2]. The reason for copper's biological importance lies in its ability to exist in two stable oxidation states — specifically, 1+, also referred to as the cuprous state, and 2+, also referred to as the cupric state. This property allows copper to mediate one-electron exchange reactions, which are

crucial components of nutrient metabolism, as well the "respiratory burst", a free radical-mediated defense mechanism against infection [3]. Additionally, copper is a known cofactor required for the proper functioning of dozens of metalloproteins [4]. This capacity to participate in one-electron exchanges can be "double-edged sword" for organisms relying on it however, as copper is both a potent generator and suppressor of radical species [3].

1.2 Human Copper Metabolism and Homeostasis

As is the case with all other living things, copper is required for the survival of humans as well. After intake, dietary copper, which typically exists in the cupric state, must first be reduced to the cuprous state by membrane-bound metalloreductase proteins found in the cells that line the duodenum, as well as the stomach, to a lesser extent [5]. These reductases are known as the Six-Transmembrane Epithelial Antigen of Prostate, or STEAP family of proteins. Another membrane protein, known as Duodenal Cytochrome B, or DCYTB, has also been proven to function as a copper reductase *in vitro*, although it is not currently known with certainty if it performs this function *in vivo* [6]. After reduction to the cuprous state, copper is then transported from the intestinal lumen into the enterocytes, primarily by Copper Transporter 1 (CTR1), as well as CTR2, to a lesser extent [7]. It is important to note that upon copper uptake by a cell, the ion is immediately bound by one of several carriers to prevent unwanted reactions with cellular components, which may generate free radical species [8]. Some copper is bound in the enterocyte by metallothionein (possibly after being delivered by glutathione, another copper carrier), where it is then shuttled to several secondary carriers within the cell, and eventually to its final destination. One these secondary carriers is known as Copper

Chaperone Protein, or CCS, which in turn shuttles the copper ion to Cu/Zn Superoxide Dismutase (SOD1), a protein necessary for the suppression of reactive oxygen species within the cytosol [7]. Another is Cytochrome C Oxidase copper chaperone, also known as COX17, which delivers copper to the mitochondria, where it is incorporated into Cytochrome C Oxidase, a critical protein required for cellular respiration [8].

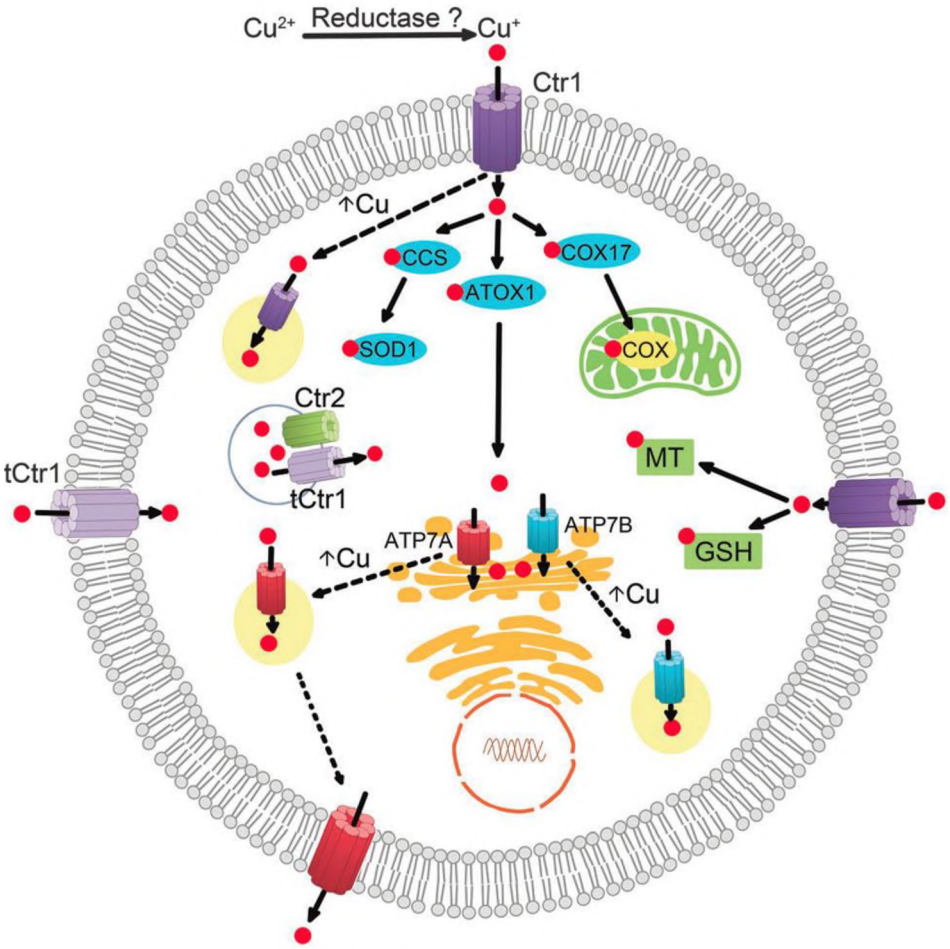

Figure 1.1 — Copper homeostasis in mammalian cells. Environmental copper, almost always found in the cupric state, is first reduced by a reductase protein found on the membrane of the cell, notably STEAP2, STEAP3, and STEAP4. After reduction, copper is transported through the membrane by Copper Transporter 1 (CTR1) into the cytosol, where it quickly binds to one of several chaperone proteins. CCS shuttles copper ions to the radical-quenching enzyme superoxide dismutase 1 (SOD1). COX17 delivers the copper ion to the mitochondria, where it can be incorporated into Cytochrome C Oxidase, which participates in the electron transport chain. ATOX1 shuttles copper to the trans-

Golgi network, where it can be transported out of the cell to another destination in the body. Additionally, copper ions may also bind to metallothionein or glutathione, which store the ion while preventing it from oxidizing other components of the cell. Source: Denoyer, D., *et al.* Targeting copper in cancer therapy: 'Copper That Cancer', Metallomics. 2015; 7:1459-1476.

Most uptaken copper, however, is shuttled to the trans-Golgi network by Antioxidant Protein 1 (ATOX1, also known as HAH1), where it is then taken up into the Golgi body by a P-type ATPase known as ATP7A [9]. This ATPase is also referred to Menkes's Disease protein, or MNK, as it is the transporter that is dysfunctional in patients suffering from the eponymous condition. Menke's Disease is an X-linked recessive disorder characterized by systemic copper deficiency due to an inability of copper to be mobilized from enterocytes to the liver, and then on to its many destinations around the body from there [2]. MNK is also the protein responsible for maintaining normal copper levels in cells throughout the body, with the notable exception of the liver cells known as hepatocytes. Another copper homeostasis-related condition, known as Wilson's Disease, is characterized by a similar mechanism in hepatocytes, in which the corresponding P-type ATPase located on the Golgi bodies of the cells, known as ATP7B, or Wilson's Disease protein (WND), is defective, and therefore unable to excrete excess dietary copper from the liver via the biliary pathway. Copper ions, in turn, accumulate in the body's tissues, notably the liver and nervous system, and cause deleterious effects [9].

In healthy individuals, however, after being shuttled by ATOX1 and taken up into the trans-Golgi network by MNK, copper is then transported to the hepatic portal vein, where it reaches the liver [10]. Upon being taken up by CTR1 into a hepatocyte, copper ions follow largely the same pathways that they follow after being taken up by an enterocyte, as described above. However, after being shuttled to the trans-Golgi network,

hepatic copper ions then meet one of two fates – they may be sent to the biliary pathway and excreted in the feces if levels of the element are higher than what the body requires; or, copper ions may be bound by ceruloplasmin, another copper-carrying protein found primarily in the blood, and then transported to the plasma for distribution around the body [8]. Interestingly, several basic facts regarding optimal copper intake levels and humans are still unclear [11], such as what percentage of copper from the diet is absorbed (previously published studies have reported numbers between 12% - 71%), and whether excess copper intake can increase the risk of various diseases (current evidence, though far from conclusive, does not support the assertion that it does) [11]. This is largely because modern humans eat quite varied diets, and it is therefore difficult to perform sufficiently controlled experiments. It is additionally complicated by the lack of reliable biomarkers of copper exposure at the current time [12].

1.3 The STEAP Family of Proteins

When found in nature, copper typically exists in the 2+ oxidation state, rather than the less common 1+ oxidation state, or the elemental state. However, before a copper ion can be taken up by a cell from its environment, the copper ion must be in the 1+ oxidation state. Thus, mammalian cells utilize a protein family known as the Six Transmembrane Epithelial Antigen of Prostate, or STEAP, proteins. Three of these four proteins, STEAP2, STEAP3, and STEAP4, have been identified as metalloreductases, reducing extracellular iron ions from the 3+ (ferric) state to the 2+ (ferrous) state, and

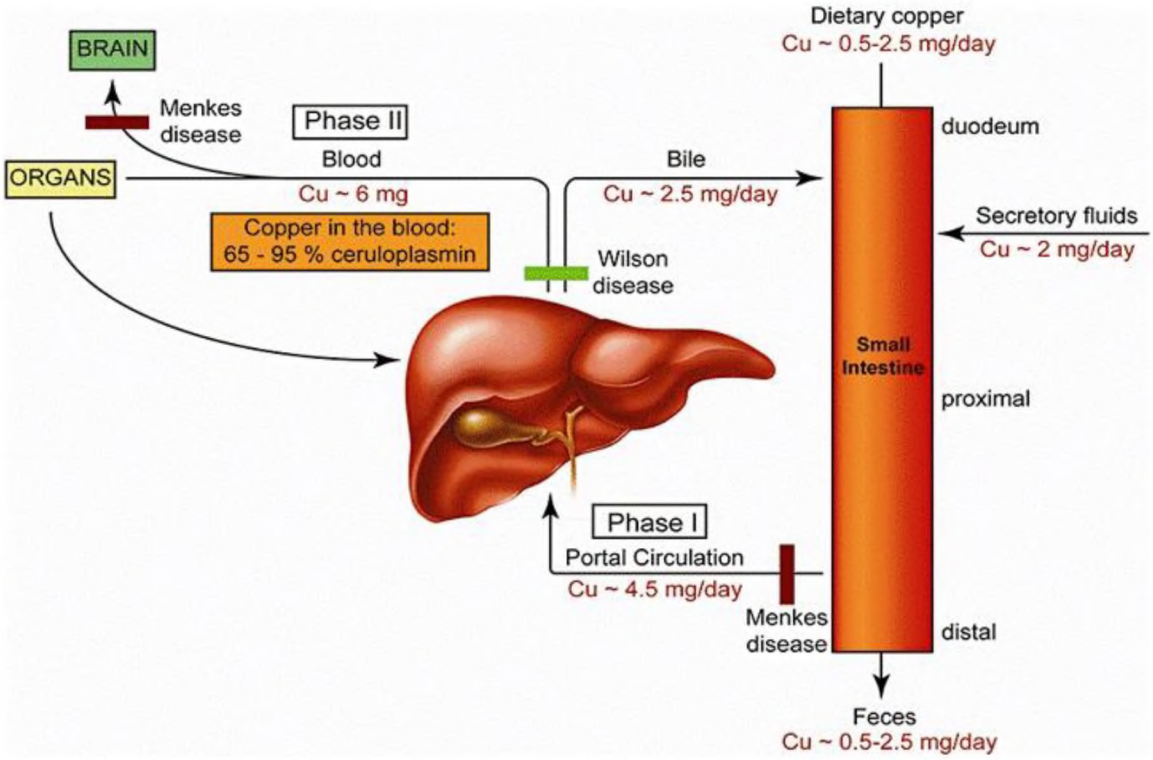

Figure 1.2 — Human copper metabolism. Copper ions are primarily absorbed into enterocytes in the lining of the duodenum of the small intestine. It is then exported to the hepatic portal vein, where it binds to one of several serum copper-binding proteins, notably ceruloplasmin and albumin. From there, the ions can either be stored in the hepatocytes of the liver, or exported to the bloodstream and other locations within the body. Excess copper is exported into the bile by the liver, where it is then removed from the body in the feces. Individuals with Menke's Disease present with a defect in the ATP7A protein, which leads to chronic copper deficiency. Individuals with Wilson's Disease suffer from a defect in the ATP7B protein, leading to copper overload in the liver, which can cause many deleterious effects through Fenton chemistry, a common mechanism mediated by copper or iron ions through which radical oxygen species can be generated. Source: Van den Berghe, P., Klomp, L. New developments in the regulation of intestinal copper absorption. Nutr Rev. 2009; 67(11): 658-672.

copper ions from the 2+ (cupric) state to the 1+ (cuprous) state, using NAD+ as an acceptor. Expression of these proteins has been observed at the mRNA level on tissues throughout the body, with the most robust expression on the fetal liver, prostate, brain, pancreas, bone marrow, and placenta [13].

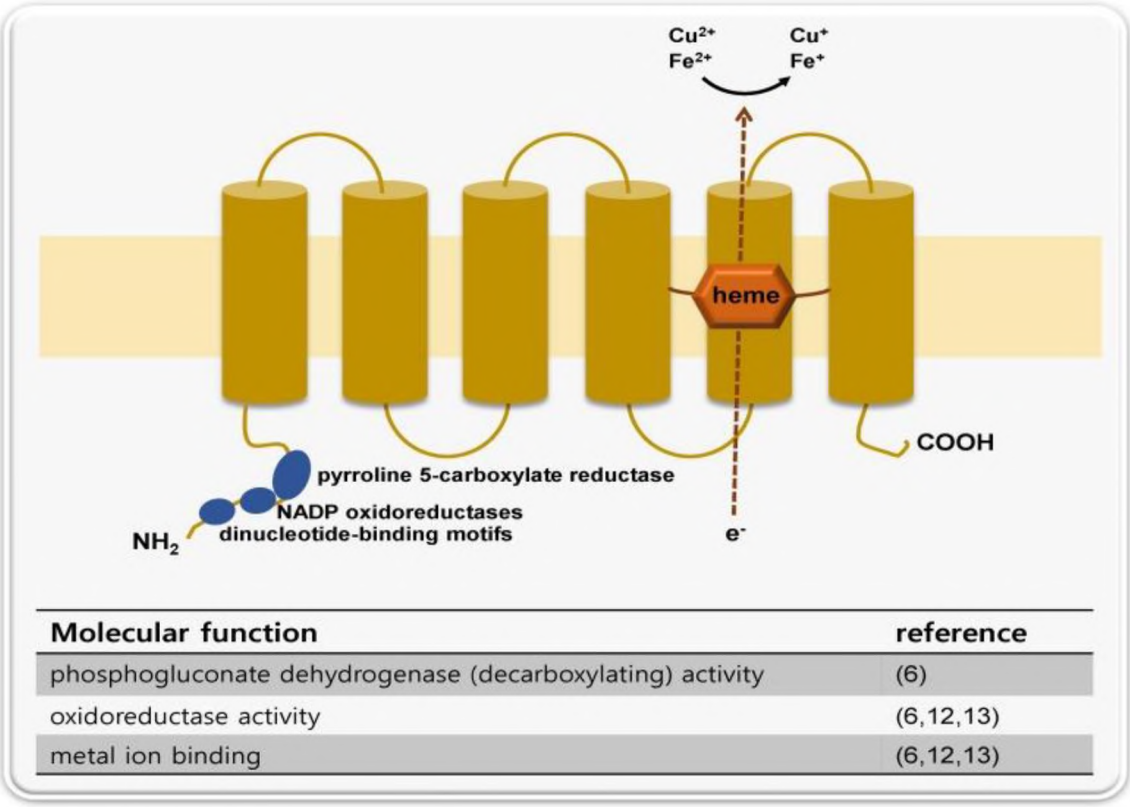

Molecular function	reference
phosphogluconate dehydrogenase (decarboxylating) activity	(6)
oxidoreductase activity	(6,12,13)
metal ion binding	(6,12,13)

Figure 1.3 — A schematic description of STEAP4's protein structure and molecular functions. STEAP4 is capable of reducing iron and copper ions, using NAD+ as an acceptor. This function requires the ability to bind metal ions. It has also been reported that STEAP4 exhibits phosphogluconate dehydrogenase activity, and is thus capable of reducing 6-phosphogluconate to ribulose 5-phosphate, using NADP as a redox partner. Source: Yoo, S., Cheong, J., & Kim, H. (2014). STAMPing into Mitochondria. Int J Biol Sci, 10(3), 321-326.

1.4 Colorectal Cancer

The colon, also known as the bowel or large intestine, is the last part of the digestive system in vertebrates, being immediately preceded by the small intestine. The colon can be divided into several sections, beginning with most proximal and ending with the most distal: cecum, appendix, ascending colon, transverse colon, descending colon, sigmoid colon, rectum, and anal canal [14]. The large intestine serves to absorb water and some nutrients from ingested food, and to move the indigestible matter along its tract and store it until the material can be excreted as feces through the anus during

defecation. The colon is also home to a large community of bacteria, known as gut flora, which subsist off of nutrients consumed by the host, and in turn aid in the process of digestion [15].

Colorectal cancer is defined as a tumor, characterized by uncontrolled, abnormal cell growth that may invade other tissues in the body, that begins in this part of the lower digestive tract. The disease arises from colorectal polyps – small growths that form in the lining of the colon and are typically benign when they are first formed. It is the third most commonly diagnosed form of cancer worldwide [16], and the second leading cause of cancer-related deaths in the United States [17]. The average risk of an individual developing colorectal cancer in his or her lifetime is approximately five percent, however this risk varies considerably between individuals based on several factors, including diet and physical activity levels, tobacco usage, family history of the disease, heavy alcohol use, and chronic intestinal inflammation (which will be discussed in more detail in a later section) [18]. Globally, colorectal cancer accounts for approximately one in ten cancer diagnoses [16], though it is significantly more common in Western countries, where it accounts for around sixty-three percent of cancer diagnoses [19]. Both sexes are approximately equally likely to be diagnosed with colorectal cancer, though men are slightly more likely to be diagnosed with rectal cancer specifically [20]. Approximately seventy-two percent of colorectal cancers originate in the colon, while the remaining twenty-eight percent originate in the rectum [17]. The median age of diagnosis of colon cancer is 68 for men and 72 for women, while for rectal cancer it is 63 years of age in both men and women [17]. It is estimated that over 1.3 million Americans are currently living with colorectal cancer [21]. Recently, it has been demonstrated that rates of

colorectal cancer in young adults have been increasing between 1.0 – 2.4% annually in adults between 20 and 39 years of age since the mid-1980s, and by 0.5 – 1.3% in adults between 40 and 54 years of age since the mid-1990s [22].

The likelihood of survival and recovery from colorectal cancer is heavily dependent upon the stage at which it is identified and diagnosed. Individuals diagnosed with the condition in stages 1, 2 and 3 all have five-year survival rates above eighty-five percent – by contrast, patients diagnosed at stage four, after distant metastases have been established, the five-year survival rate is eleven percent [23]. Because of this, survival rates from colorectal cancer have increased considerably in recent decades, rising from around fifty percent to six-four percent from 1995 to 2000 alone [19]. This is largely due to increased public awareness about the importance of regular screenings, which often catch colorectal polyps before they become malignant at all [20]. Currently, around forty percent of colorectal cancer cases are diagnosed in the local stages, compared to thirty-six percent in the regional stage and twenty percent in the metastatic stage [17]. While incidence of the disease has declined dramatically in the developed world over previous decades however, significant disparities in outcomes remain for economically and racially disadvantaged groups [24].

As mentioned earlier, many different factors influence an individual's risk of developing colorectal cancer. Some of these risk factors cannot be controlled, such as age and genetic considerations. However, many colorectal cancer risk factors are modifiable. One crucial variable that plays a role in this is diet. Diets rich in animal products such as meat and fat have been implicated in the risk of developing these

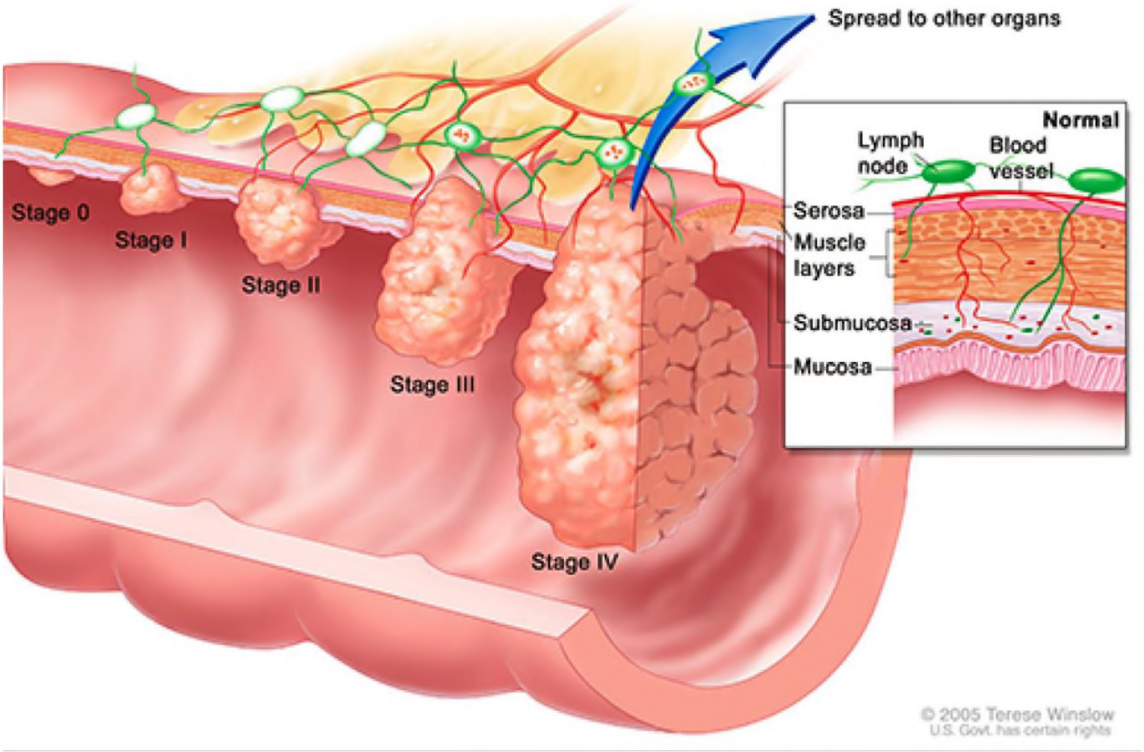

Figure 1.4 — Stages of colorectal cancer. In Stage 0 CRC, the tumor has not grown beyond the mucosal layer of the colon. In Stage 1 CRC, the tumor has grown through mucosal layer of the colon into the submucosa. In Stage 2 CRC, the tumor has grown into the muscular layer of the colon, but has not yet reached the surrounding lymph nodes. In Stage 3 CRC, tumor cells have spread to the lymph nodes surrounding the colon. Finally, in Stage 4 CRC, the primary tumor has metastasized and spread to other organs. Source: https://www.webmd.com/colorectal-cancer/ss/slideshow-colorectal-cancer-overview. For the National Cancer Institute © 2005 Terese Winslow LLC, U.S. Govt has certain rights.

diseases [18]. Possible reasons for the link between animal product consumption and colorectal cancer include the high iron content of red meat, a crucial nutrient for the development and progression of cancers, as well as dietary fat creating an environment in which gut flora capable of converting bile salts to carcinogenic *N*-nitroso compounds can thrive [19]. Consumption of fruits and vegetables are believed to mitigate the risk of colorectal cancer due to their high fiber content [25]. Another modifiable risk factor in the development of the condition is tobacco usage – it is estimated that around one in

eight cases of colorectal cancer deaths can be directly attributed to cigarette smoking [26]. Cigarette smoking is known to increase the rates of formation and growth of adenomatous polyps, which often develop into cancerous lesions [27]. Consumption of large amounts of alcohol can also increase the risk of colorectal cancer development, perhaps synergistically with tobacco smoking [28]. This has been suggested to be due to the carcinogenic metabolites of alcohol, alteration of systemic hormone levels, changes in folate metabolism, as well as alcohol-mediated oxidation of lipids and generation of reactive oxygen species. There is also some evidence to suggest that alcohol can act as solvent that increases the penetration of tobacco-derived carcinogens into colon mucosal cells [19].

Another risk factor associated with incidence of colorectal cancer is obesity and lack of physical activity. Indeed, many studies have demonstrated not only correlations between excess body fat as well as a sedentary lifestyle with risk of developing colorectal cancer, but also an inverse correlation between intensity and frequency of exercise sessions and the individual's risk of developing the disease [19]. The proposed reasons for this relationship are numerous, and include increased gut motility, enhancement of immune system function, decreasing levels of insulin and insulin-like growth factor, decreasing body fat content, enhancing free radical scavenger systems, and influencing prostaglandin levels [29].

1.5 Liver Metastasis of Colorectal Cancer

One of the reasons colorectal cancer is such a pernicious disease is its tendency to form distant metastases, often in the liver [30]. When nutrients from food are absorbed from the lumen of the intestines into the bloodstream, the nutrient-rich blood is

immediately transported from the gastrointestinal tract to the liver via a large vein known as the hepatic portal vein. This allows the nutrients, as well as any xenobiotics that were ingested, to be at least partially metabolized before entering systemic circulation. It also, however, provides a direct transportation route for malignant cells from the intestines to travel to the liver as well. Additionally, the liver is the body's primary site of copper storage, which could potentially contribute to the high frequency of successful metastases from the intestines that establish in that organ. Epidemiological evidence suggests that approximately fifteen percent of colorectal cancer patients experience a synchronous liver metastasis at some point during their lives [31]. Additionally, around twenty percent of individuals diagnosed with colorectal cancer receive their diagnosis after the primary tumor has metastasized [32]. Among this group, the five-year survival rate is a bleak eleven percent, compared to a rate of above eighty-five percent for individuals diagnosed before a distant metastasis occurs.

In recent decades, a significant body of evidence has emerged that implicates pro-inflammatory signaling pathways in colorectal tumor metastasis, as well as in tumorigenesis and progression [32]. Indeed, different types of immune cells, which can mediate different immune signaling pathways, are alternatively associated with both tumor-suppressing and tumor-promoting microenvironmental conditions. For example, several different types of cancers, when highly infiltrated by tumor associated macrophages (or TAMs), are generally characterized by poor prognosis; however, in colorectal cancer, tumors that present with elevated levels of T cells are associated with decreased mortality rates [33]. The most important factor that defines whether a particular immune cell type is associated with a tumor-suppressing or tumor-promoting

microenvironment is the cytokines that particular cell type is known to secrete and be activated by. One particular signaling pathway activated by IL-17 that has been demonstrated to play an important role in cancer progression is known as nuclear factor kappa-light-chain-enhancer of activated B cells, or the NF-κB pathway [34]. A protein complex known to regulate DNA transcription and the production of cytokines, NF-κB can be activated by a wide array of different ligands, including endogenous cytokines as well as exogenous molecular patterns associated with invading pathogens. NF-κB signaling controls the expression of several genes relating to cell survival and proliferation, and is known to be a response to various harmful stimuli such as free radicals, cytokines, bacteria, viruses and others [35]. Published literature has specifically implicated the robust activation of NF-κB signaling in liver metastases of colorectal cancer as well [36].

1.6 MAPK/ERK Signaling and Cancer

Being a disease characterized by abnormal, uncontrolled cell proliferation, many different growth pathways play an important role in cancer progression. One of these key signaling pathways is the MAPK/ERK pathway, named for the mammalian family of Mitogen-Activated Protein Kinases. Three MAPK families have been well-characterized in mammalian cells, known as the classical MAPK pathway (also known as the ERK pathway), C-Jun N-terminal kinase/stress-activated protein kinase (also known as JNK/SAPK), and p38 kinase. In these cascades, an extracellular signal (hence the ERK designation – Extracellular-signal Regulated Kinases) binds to a tyrosine kinase receptor on the surface of the cell, which, in turn, provokes the activation of MAPKs through a multistep process, made up of no fewer than three enzymes that are activated

sequentially. These pathways amplify signals from a wide range of stimuli, and are capable of causing cell growth, proliferation, differentiation, inflammatory responses, and apoptosis [37].

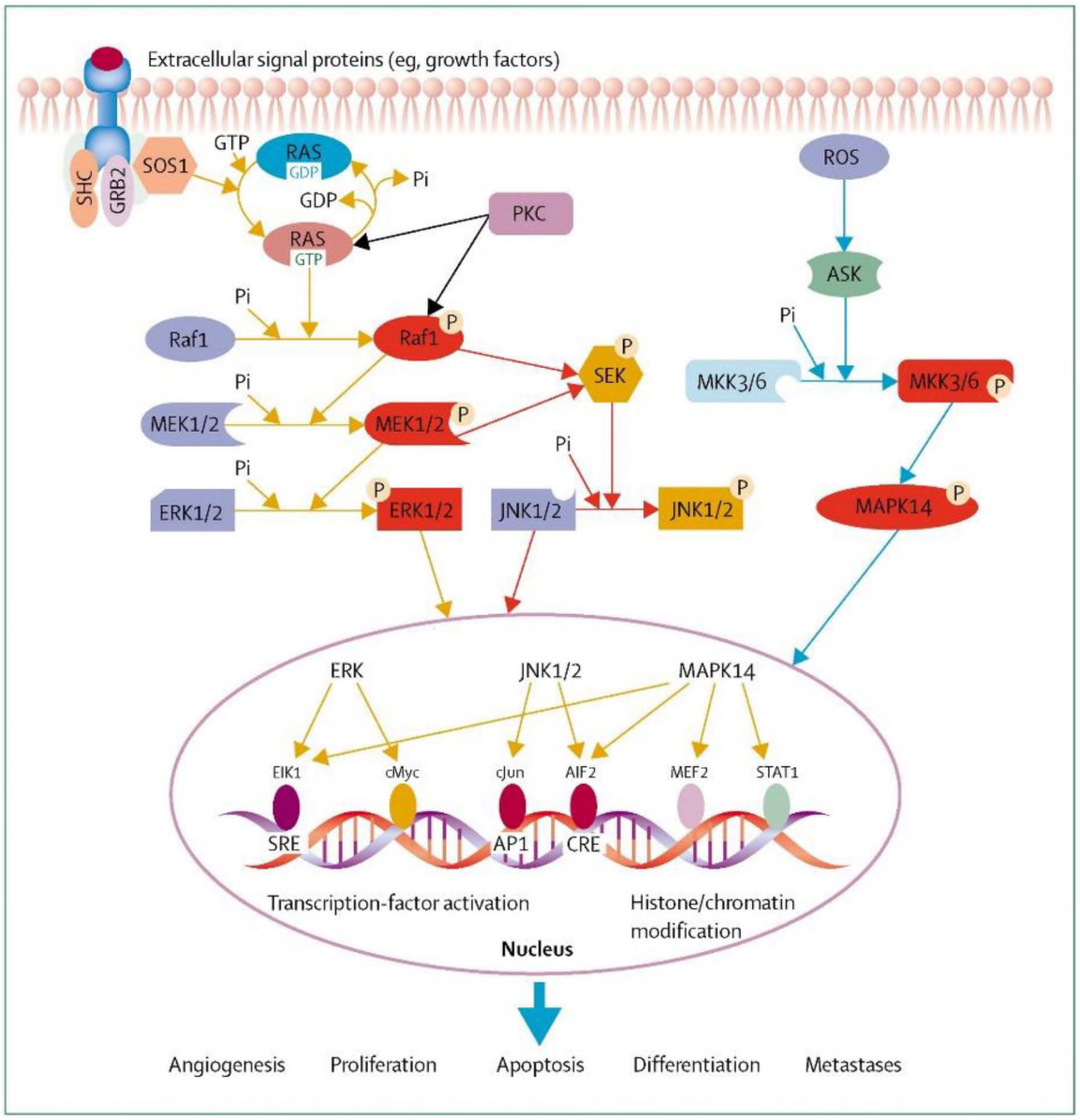

Figure 1.5 — MAPK/ERK signaling in the pathogenesis of cancer. One of numerous extracellular signaling molecules first binds to its receptor. A number of downstream proteins are phosphorylated in a sequential process, eventually leading to the activation of ERK1/2, JNK1/2, or MAPK14, which then enters the nucleus of the cell and activates transcription factors or modifies DNA-supporting proteins, thus leading to alteration of gene expression. Source: Fang, J., & Richardson, B. (2005). The MAPK signalling pathways and colorectal cancer. Lancel Oncol, 6(5), 322-327.

Being involved in stimulating cell growth and proliferation, it should come as no surprise that dysregulation of the MAPK/ERK pathway has been implicated in many different types of cancer [37]. Indeed, ERK signaling has been shown to play a significant role in several events related to tumor development. These include promotion of cancer cell migration, induced expression of matrix metalloproteins that promote the degradation of the extracellular matrix, and hence tumor invasion, and regulation of several proteins involved in apoptosis, which, in turn, promote cancer cell survival [38]. Consequently, the ERK receptor is considered to a robust target for anti-cancer therapeutic development. Additionally, it has previously been noted that mutations in the Epidermal Growth Factor Receptor (EGFR), which activates the ERK pathway, have frequently been observed in colorectal cancers [39].

1.7 Copper Chelation as Anti-Cancer Therapy

As it has now been well-established that copper is crucial for cancer progression, copper depletion strategies have since become a promising approach for new cancer therapies. Chelation is defined as when multiple coordinate bonds form between a polydentate ligand and a central atom, which are almost universally metals [40]. Upon chelation, the central reactivity of the central atom is reduced, as it is both coordinated with a ligand and physically separated from the competing ligands that may be capable of coordinating with the central atom. Before its research application to cancer, copper chelation therapy had previously been used to treat Wilson's Disease patients, who experience systemic copper overload, particularly in the liver and brain. Therefore, several chelators that were known to be well-tolerated were already in usage, such as

ammonium tetrathiomolybdate, as well as several others [41]. As mentioned previously, copper is a critical element required for the process of angiogenesis – the generation of new blood vessels required for tumor growth and metastasis. Additionally, an emerging body of evidence suggests that copper can directly promote cancer metastasis as well. Thus, a number of studies [42] have reported that copper depletion through chelation therapy is a promising strategy for treating various forms of cancer, and it is highly likely that research into this direction will continue into the future.

1.8 Inflammation and Cancer

One of the most significant risk factors for developing colorectal cancer, and many other types of cancers as well, is the presence of chronic inflammation [32]. Inflammation is an innate immune response against a pathogen, abnormal cell, injury or chemical irritant characterized by red appearance of the inflamed area, pain, swelling, and loss of function [43]. The components of inflammation include vasodilation, increased permeability of blood vessels, invasion of white blood cells into the affected tissue, as well as a number of complex signaling cascades. The acute inflammatory response is initiated by immune cells present within the affected area such as macrophages and dendritic cells, among others. Upon encountering the harmful stimulus, these cells, which contain pattern recognition receptors, or PRRs, on their surfaces, bind to the stimulus and are activated, and then begin releasing various pro-inflammatory mediators. These mediators are in turn responsible for the clinical signs and symptoms of inflammation and can be broken down into many different categories such as cytokines, chemokines, enzymes, interferons, and others. The large variety of

these mediators allows inflammation to fight effectively against a wide range of pathogens [44].

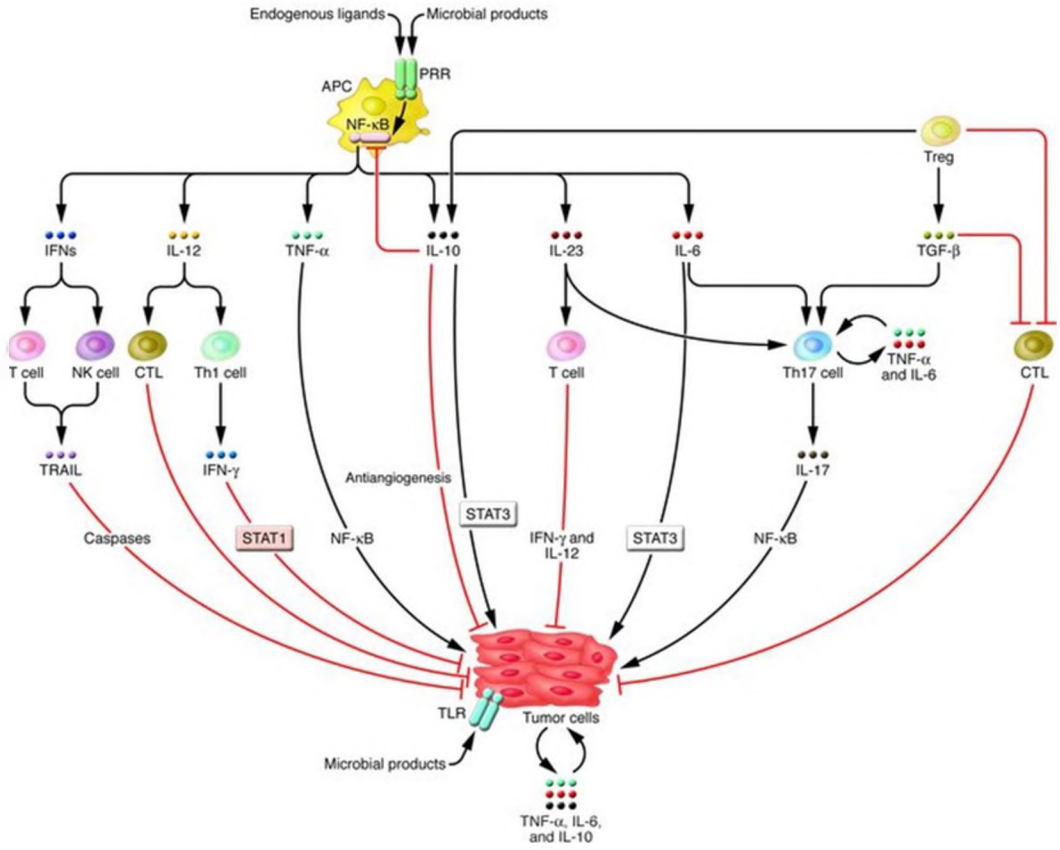

Figure 1.6 – Immune system signaling and inflammation play a critical role in the risk of tumorigenesis and cancer progression. Upon recognition of a pathogen by the host's immune system via presentation by an APC, a variety of cytokines, both pro-inflammatory and anti-inflammatory, are released by myeloid cells. These cytokines bind directly to tumor cells and affect their behaviors relating to cell growth, proliferation, and invasion, and also regulate the activities of other immune cells, such as regulatory T cells, TH-1 cells, TH-17 cells, and Natural Killer cells. Critical cytokines that affect tumor cell behavior include IFNγ, IL-6, IL-10, IL-17, IL-12, IL-23, TNFα, and TGFβ. Source: Karin, M., Lin, W. (2007). A cytokine-mediated link between innate immunity, inflammation, and cancer. J Clin Invest, 117(5), 1175-1183.

While the acute inflammatory response has a beneficial defensive effect against the initiator of the response, chronic inflammation can lead to many negative consequences in the affected individual. Chronic inflammation can be distinguished from its acute counterpart not only by the length of the response, but also by the actions of the

cells and molecules involved. For example, T lymphocyte infiltration into the affected tissue is observed in cases of chronic inflammation, but not in the acute response [43]. The entire pathology of inflammation is remarkably complex, and an exhaustive description is beyond the scope of this thesis. However, one well known consequence of chronic inflammation is an increased risk of cancer in the affected tissue. Indeed, over twenty percent of individuals diagnosed with inflammatory bowel disease will be diagnosed with colorectal cancer within thirty years of IBD onset, and more than half of these patients will eventually die from the cancer. Additionally, many colorectal tumors display increased activity of various pro-inflammatory biochemical pathways, providing further evidence of the underlying connection between the two conditions [32].

The exact reasons for why chronic colitis increases an individual's risk of development of colorectal cancer are not fully understood. However, various characteristics of inflammation have been implicated in all stages of cancer advancement, including tumorigenesis, tumor progression and metastasis. One important molecule that is known to impact inflammation and its effects on cancer is interleukin 17, also known as IL-17. IL-17 is a pro-inflammatory cytokine produced by helper T cells, known as Th17 cells, as well as immune sentinel cells, that is known play a critical role in regulating the innate immune response [45]. Specifically, IL-17 is known to induce IL-6, IL-8, and several other pro-inflammatory mediators. IL-17 is also known to be a potent direct activator of neutrophils, as well as several genes that serve anti-microbial functions. However, this activity also makes IL-17 crucially important in the pathology of autoimmune disorders, such as psoriasis, rheumatoid arthritis and systemic lupus erythematosus. This pro-inflammatory activity has also implicated IL-17 in contributing

to an environment in which tumors can thrive [46]. Interestingly however, and in an illustration of the "double-edged sword" that is the inflammatory response, where it can defend a host against foreign threats but can also cause self-damage, some papers have also reported that IL-17 can protect against cancer growth and metastasis by enhancing the anti-tumor activity of the immune system [47].

1.9 The Interleukin-17 Signaling Pathway

The existence of IL-17, originally named CTLA8, was first reported in 1993 when its messenger RNA (mRNA) transcript was isolated from a rodent T cell hybridoma [48]. It was subsequently discovered that the IL-17 family of cytokines consists of several different molecules, termed IL-17A (often referred to simply as IL-17), IL-17B, IL-17C, IL-17D, IL-17E (also known as IL-25), and IL-17F. These cytokines are all considered to be members of the same family because they all exist as homodimers and share five highly conserved cysteine residues is their C-terminal region that are crucial for the three-dimensional structure of the proteins [49], and their genetic coding information is located in humans on chromosome 6. The IL-17 family of cytokines bind to receptors known, quite logically, as the IL-17 receptor (IL-17R), which consist of several variants. These variants are all oligomers, most commonly dimers, which are all comprised of different combinations of three monomeric subunits, known as IL-17RA, IL-17RB, and IL-17RC [50]. IL-17A, which shall henceforth be referred to simply as IL-17, consists of 155 amino acid residues and has a molecular weight of 35 kDa [51]. Helper T cells (also known as CD4+ T cells) that produce IL-17 are known as TH-17 cells. Naïve T cells can be differentiated into a TH-17 lineage upon stimulation with several different ligands, including transforming growth factor beta (TGF- β), IL-6, and IL-23 [52]. Like other

CD4+ cells, TH-17 cells are activated after an antigen presenting cell (APC), such as a macrophage, ingests an invading pathogen and presents a fragment of a peptide from that antigen on a specialized surface protein, known as a class 2 major histocompatibility complex (MHC). The antigenic peptide fragment bound to the class 2 MHC on the surface of the APC then binds to the CD4 protein on the surface of the helper T cell, thus activating the T cell and causing it to begin releasing its signature cytokine [53]. In the case of TH-17 cells, this signature cytokine is, unsurprisingly, IL-17, though TH-17 cells also produce and secrete IL-22 [54].

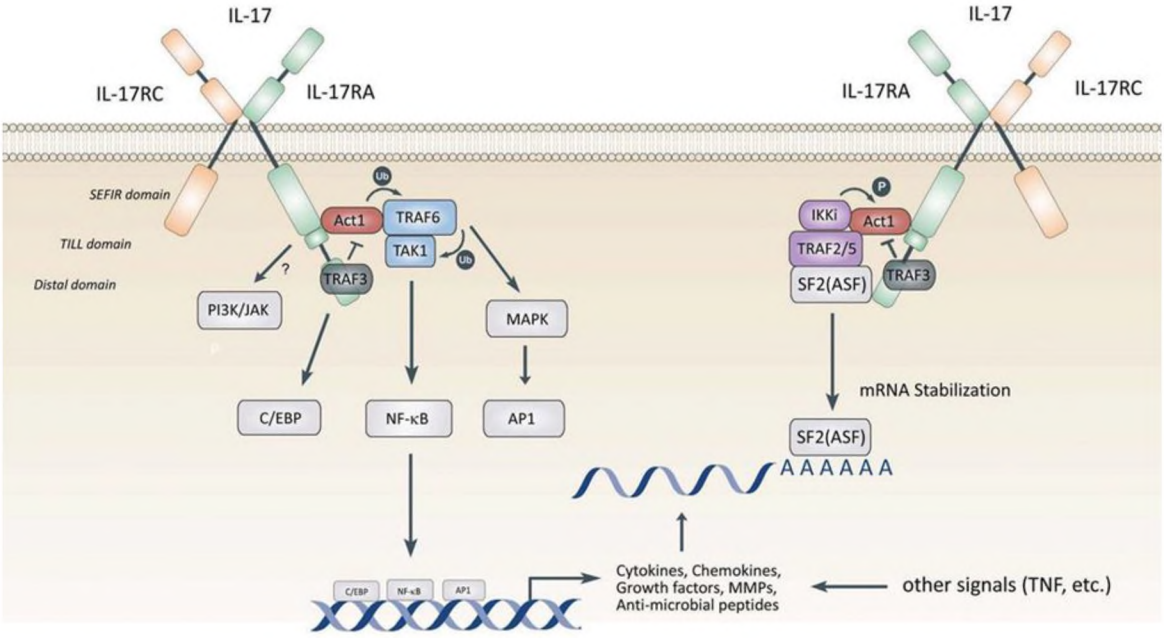

Figure 1.7 – IL-17 increases expression of many genes through activation of various downstream signaling pathways. IL-17A, commonly referred to as IL-17 without qualification, exists as a heterodimer. IL-17 binds to the IL-17 receptor complex, referred to as IL-17R, forms a homodimer consisting of one IL-17RA subunit and one IL-17RC subunit upon ligand binding. Both subunits of IL-17R possess a SEFIR domain, which recruits Act1 upon activation of the receptor complex. Act1 can then bind to TRAF6, and also acts as an E3 ligase that ubiquitinates TRAF6. TRAF6, in turn, acts as an E3 ligase and ubiquitinates TAK1, which can then directly activate the NF-κB pathway. The Act1-TRAF6-TAK1 pathway can also activate the MAPK/ERK and C/EBP signaling pathways. IL-17R can also activate the PI3K/JAK pathway through a yet unknown mechanism. Additionally, TRAF3 can act as a negative regulator of IL-17R activity. Additionally, activated IL-17R can also form an Act1–IKKi–TRAF2–TRAF5–SF2(ASF)

complex that promotes mRNA stability and increases expressions of genes induced by IL-17. Source: Source: Zhu, S., Qian, Y. (2012). IL-17/IL-17 receptor system in autoimmune disease: mechanisms and therapeutic potential. Clin Sci, 122(11), 487-511.

IL-17 signaling plays many important roles in immune system function, particularly those related to host defense against bacteria and fungi. IL-17R is found abundantly on various types of cells in mucosal barriers, such as epithelial cells and fibroblasts [55]. These mucosal barriers line areas of the body that are exposed to the outside world, such as the skin, gastrointestinal tract, nasal cavity, urinary tract, and reproductive tract, as well as others. Upon stimulation of IL-17R by a ligand, the target cell begins producing antimicrobial peptides, such as β-defensins, S100 proteins, and regenerating islet-derived protein 3g (ReG3g), which function as endogenous antibiotics through mechanisms such as disrupting prokaryotic membranes and interfering with the function of critical bacterial cellular processes [56]. The other main function of IL-17 signaling involves sustaining a pro-inflammatory response. IL-17 stimulation of cell has been reported to increase expression of other pro-inflammatory cytokines, such as IL-1β, IL-6, GM-CSF, G-CSF and TNFα from many types of cells, including fibroblasts, macrophages, chondrocytes and osteocytes [57]. IL-17 additionally stimulates increased expression of many chemokines which recruit leukocytes to the stimulated tissue. These include CCL2, CCL7, CXCL1, CXCL2, CXCL5 and CXCL8, which recruit neutrophils and monocytes from the bloodstream, CCL20, which recruits additional IL-17-producing immune cells, and CXCL9 and CXCL10, which further recruit leukocytes to the affected tissue. An additional way that IL-17 promotes recruitment of immune cells to the target tissue is through promotion of vasodilation and activation of tissue remodeling genes. Cells stimulated with IL-17 may undergo structural changes in their extracellular

matrices through modification of the expression of several different matrix metalloproteinases. Through these various mechanisms, IL-17 sustains a pro-inflammatory environment [57].

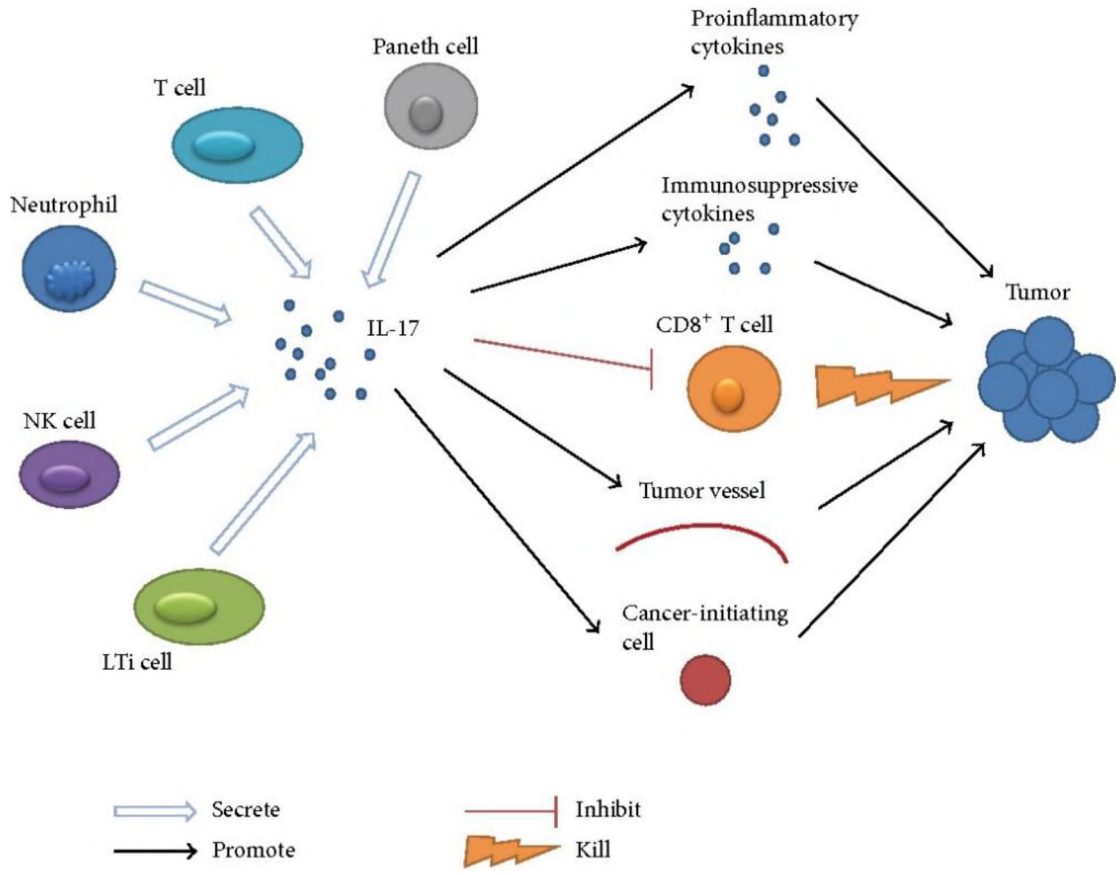

Figure 1.8 — IL-17 and the pathogenesis of cancer. Upon stimulation by a pathogen, one of many different immune cells, including Paneth cells found in the epithelium of the small intestine, begins secreting IL-17. This has a number of tumor-promoting effects, including stimulating the release of other cytokines from target cells, inhibition of cytotoxic T cells, and promotion of tumor-initiating cells and tumor vessels. Source: Wu, D. (2013). Interleukin-17: A promoter in colorectal cancer progression. Clin Dev Immunol.

However, this type of positive feedback response has a significant drawback – namely, that sustained activation of IL-17 signaling has been implicated in many different autoimmune disorders. Autoimmune diseases are a broad class of disorders characterized by an immune response by a host against the body's own cells and tissues.

Common autoimmune disorders include Systemic Lupus Erythematosus (SLE), Rheumatoid Arthritis (RA), Type 1 Diabetes Mellitus, Multiple Sclerosis (MS), and, most relevant to this thesis, Inflammatory Bowel Disease (IBD). While the pathogeneses of these diseases are not fully understood, it is believed that IBD is caused by an abnormal immune response against the gastrointestinal microbiota. Previous reports have shown that IL-17 expression is increased in the mucosa of the large intestine as well as the serum of IBD patients compared to normal patients [58]. Further studies have confirmed through animal models that IL-17 signaling plays a crucial role in the pathogenesis of IBD [59]. However, given the current body of evidence relating IL-17 and IBD, it is still unclear whether the cytokine has disease-promoting effects or protective effects against the disease, or both, as it has been shown that both animal models of IBD in which IL-17 production was decreased or knocked out entirely, and human patients treated with anti-IL-17 drugs, displayed exacerbated symptoms, rather than relief from them [60].

1.10 Animal Modelling of Colon Inflammation and Cancer

Many animal models of colitis and colorectal cancer have been developed by researchers seeking to study these diseases. These models can be characterized according to several variables, such as the method by which the disease is introduced to the animal, and whether a cancer model is likely to metastasize. One category encompasses models in which the animals are genetically modified to spontaneously develop tumors. For example, mouse models of colorectal cancer can be created by generating specific mutations, such as those that affect the WNT signaling pathway, or DNA mismatch

repair proteins. Various other genes that may be modified include p53, KRAS, SMAD3, and others that are frequently mutated in clinical cases of colorectal cancer [61].

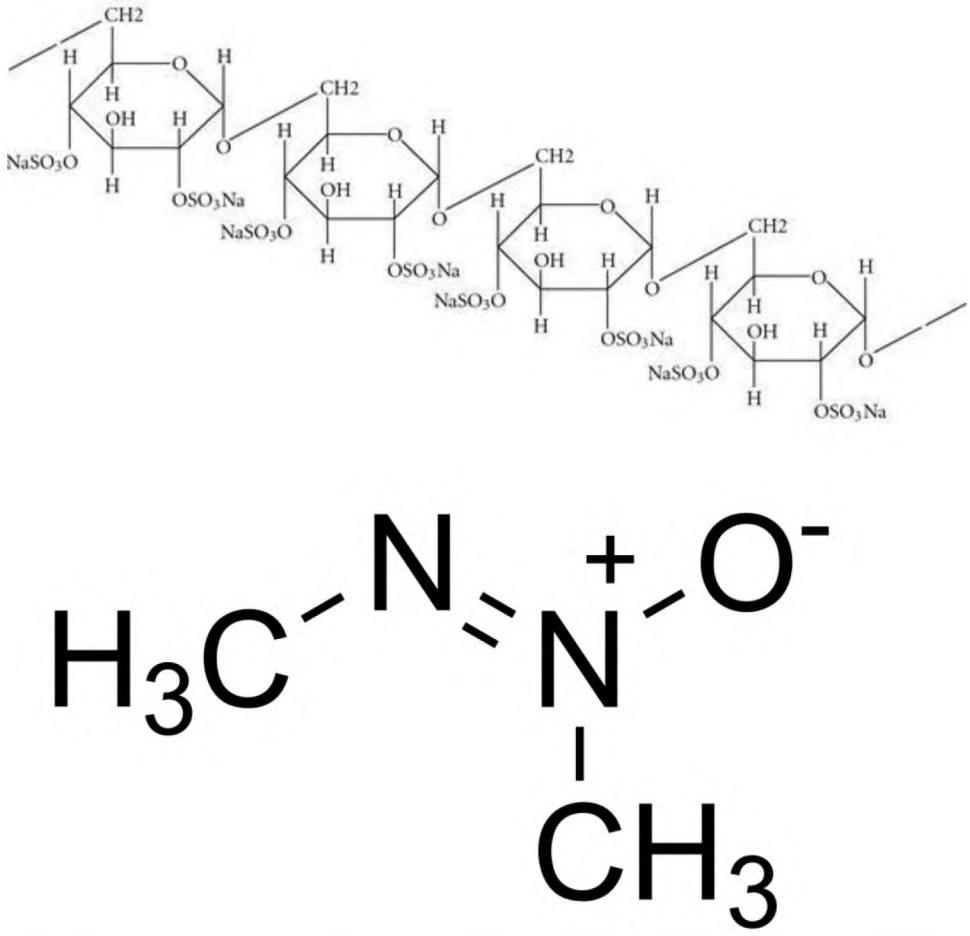

Figure 1.9 – Molecular structures of dextran sodium sulfate (DSS) and azoxymethane (AOM). AOM reliably induces colon carcinoma after intraperitoneal (IP) injection. It is therefore often used for this purpose in animal model experiments. It is believed that the mechanism of AOM-induced carcinoma involves inducing DNA base pair mismatches or disrupting normal mismatch repair mechanisms. Similarly, DSS reliably induces colon inflammation when delivered as an aqueous drinking water solution, and is often used in animal model experiments for this purpose. It is believed that DSS achieves this by acting as detergent that disrupts the normal mucosal lining of the colon, allowing gut flora to penetrate into the submucosal and muscular layers of the colon, thus generating an immune response. Source (DSS): Tanaka, T. (2011). Development of an Inflammation-Associated Colorectal Cancer Model and Its Application for Research on Carcinogenesis and Chemoprevention. Int J Inflam, 2012. Source (AOM): Wikimedia Commons.

Another broad category of colorectal cancer animal models are those that are chemically induced. The most commonly used colon inflammation model is the dextran sodium sulfate, or DSS model, in which the animal's drinking water is replaced with a dextran sulfate sodium solution, for either one or multiple cycles, punctuated by "recovery" cycles of unaltered drinking water. While the exact mechanism by which DSS administration induces colitis is not fully understood, it is believed that the chemical degrades the mucosal barrier of the large intestine by acting as a detergent, leading to infiltration of gut bacteria into the lining of the colon, which provoke an immune response [62]. Other colon inflammation models used include rectal administration of 2,4,6-trinitrobenzenesulfonic acid, or oxazolone dissolved in ethanol (which is required to penetrate the mucosal barrier.) While some animals that experience intestinal inflammation do spontaneously develop tumors at an increased rate, these models are typically combined with a one-time administration of azoxymethane (AOM), which reliably induces colorectal adenocarcinomas, most likely by causing the mismatching of nucleotide base pairs during DNA replication [63].

1.11 Engineering Recombinant Cell Lines and Proteins

For well over a century now, cells grown *in vitro*, or outside of the organism from the cells were derived, have been an invaluable tool for biological research. While whole organs isolated from animals were maintained in media containing ions and molecules necessary for life in the 19th century, research in cell culture took major steps forward in the mid-20th century, which allowed cell monolayers to be grown, for which the 1954 Nobel Prize in Medicine was awarded [64]. In modern times, a large assortment of

different cell growth media exists, capable of sustaining virtually any type of cell imaginable.

For certain experiments, in which a researcher is interested in investigating the function of a particular protein, the gene corresponding to that protein may be overexpressed, knocked out, or knocked down in a cell line. Due to the nature of the experiments detailed in this thesis, overexpressed cell lines shall be described. The introduction of purified, or "naked" DNA into a eukaryotic cell is known as a transfection. This is in contrast with performing the same action on a prokaryotic cell, which is typically called a translation. Expression of a gene may be induced either stably, where the foreign nucleic acid is integrated into the nuclear DNA of the transfected cell, or transiently, in which the transfected DNA remains in the cytosol. After purification of the DNA, there are several methods which may be used to transport the DNA across the cellular membrane. These methods may be classified as biological, chemical, or physical in nature, and include techniques such as using a viral vector, use of calcium phosphate, a cationic lipid or polymer vector, electroporation, sonoporation, laser irradiation, or use of magnetic nanoparticles [65]. Biological methods, such as introduction of DNA using a viral vector, are efficient and commonly used for experiments in which stable gene expression is desired, as they take advantage of the natural ability of viruses to integrate their genetic material into the genome of a host. They carry the significant downside, however, of potentially evoking an immune response from the host cell. Chemical methods take advantage of positively charged vectors, such as cationic lipids or cationic polymers, which are attracted to the negatively charged lipid bilayer of the cell. While the exact mechanism by which the nucleic acids

pass through the cell membrane is not fully understood, it is believed to be endocytotic or phagocytotic in nature. While these chemical methods do not carry the risk of generating an immune response, they are considerably less efficient than viral vectors and may damage the cells. Finally, physical methods, such as sonoporation, laser-based transfection, and electroporation, utilize these tools to generate holes in the cell membranes which allow the nucleic acids to travel through. Similarly to chemical methods, physical methods do not evoke an immune response in the host cells, but are less efficient than biological methods and may damage the cell.

After the purified DNA is transported into the host cell, if it is transiently expressed, target gene expression will decrease exponentially in each subsequent generation due to dilution of the genetic material in daughter cells following mitosis, and is typically only observable for several days [66]. Thus, for most experiments in which overexpression of a gene is to be investigated, a stable transfection is required. In addition to the gene of interest, a "marker" gene must be co-transfected into the cell as well, typically one that confers resistance to an extracellular toxin. This allows the researcher to specifically select for clones of cells that have integrated the foreign DNA, consisting of the both gene of interest and the marker gene, into their genome, as only clones of cells which have done so will survive in culture after addition into the medium of the toxin to which the stably transfected cells are now resistant due to expression of the marker gene. Additionally, a target gene may be modified, or "tagged", by addition of a nucleotide sequence to the complementary DNA (cDNA) of the gene that is to be expressed, which causes the gene to manufacture that specific amino acid sequence in addition to its normal amino acid sequence during protein construction. Tags allow for

use of antibodies that bind to that specific amino acid sequence within the recombinant gene, which allows a researcher to purify the desired protein by an affinity technique, as well as to quantify expression level of the protein it by Western blotting. Commonly used protein tags include the polyhistidine tag, the FLAG tag, the glutathione s-transferase tag, as well as others [67].

Further, to eliminate the complicating variables of how modifying the genome of a cell line may affect its normal behavior compared to the unmodified cells, "inducible" cell lines are often generated. One common mechanism by which this is accomplished is through the tetracycline-controlled transcriptional activation method, which allows a researcher to either provoke (termed "Tet on") or block (termed "Tet off") expression of the gene of interest in the cells via addition of the antibiotic tetracycline, or a derivative antibiotic, such as doxycycline, to the growth medium [68]. These tetracycline-inducible systems make use of a recombinant protein generated from the tetracycline repressor protein, originally discovered in *E. coli*, which prevents expression of tetracycline resistance-related genes when bound to its operator, fused with a fragment of another protein known as a transactivation domain, which provides scaffolding that allows RNA polymerase to bind to the promoter region of the DNA, and thus initiate transcription of the genes controlled by the promoter. In the case of a Tet on system, the tetracycline-binding domain of this recombinant protein binds to a tetracycline molecule, thus changing the conformation of the protein in such a way that allows it to bind to its operator [68]. After the recombinant protein has bound to its operator segment of DNA, the transactivation domain of the recombinant protein then enables RNA polymerase to bind to the promoter region of the DNA, which in turn leads to expression of the gene or

genes controlled by that promoter. The operator, promoter, and genes controlled by those segments of DNA are collectively referred to as an operon. Similarly, in the case of the Tet off system, the tetracycline-binding region of the fused protein is mutated such that tetracycline binding changes its conformation in a way that causes it to detach from its operator, thus preventing the binding of RNA polymerase to the promoter, mediated by the transactivation domain of the recombinant protein, and subsequent expression of the genes within the operon [68]. These types of systems have been in use for many years, and it has been demonstrated that these systems can be used to generate stably transfected, inducible human cell lines [69]. However, the use of tetracycline-inducible cell systems does carry the risk of altering cell metabolic processes and proliferation through exposure to doxycycline [67].

1.12 Determination of Metal Content in Solution by AAS

An effective method of determining the concentration of metals in a solution is atomic absorption spectroscopy, also known as AAS. In use since the 1950s, AAS instruments follow the general procedure of forcing the sample into the gas phase and atomizing it with some form of heat energy, then passing light of a wavelength specific to the element being determined through the atomized sample, and then measuring how much of the light is absorbed by the sample, which corresponds directly to the concentration of that element in the solution [70]. Two common methods of sample heating and atomization are by aspirating the sample into a flame, known as flame atomic absorption spectroscopy (FAAS), and alternatively by heating the sample in a small furnace made of graphite, which is known as graphite furnace atomic absorption spectroscopy (GFAAS).

CHAPTER II

EXPERIMENTAL AIMS AND PROTOCOLS

2.1 Project Rationale and Overall Hypothesis

In 2015, unpublished data from the Li Lab, seeking to identify genes whose expression in keratinocytes was upregulated after three hours of stimulation with IL-17, was generated from a quantitative proteomic analysis. This analysis revealed a that a of significant number upregulated genes were copper-related — most notably, STEAP4. From this data, it was hypothesized that the mechanism by which IL-17 signaling sustains a pro-inflammatory, tumor-promoting response may be dependent upon copper metabolism, and STEAP4 activity specifically. Prior to the generation of this data, no copper or STEAP4-dependent mechanism had ever been described in the published literature.

Symbol	log_2 Ratio (IL-17-3h/Untr-3h)	Regulated Up or Down?	P-value	FDR
Lox	0.19363	Up	0	0
Loxl2	0.191213	Up	8.37E-102	1.45E-99
Loxl1	0.035404	Up	0.000238	0.001449
Loxl3	0.005426	Up	0.598932	0.68446
Loxl4	0.158363	Up	9.21E-56	1.54E-54
Steap4	4.008474	Up	8.99E-68	1.07E-65
Cp	2.162976	Up	9.31E-183	2.99E-180

Table 2.1 – Many copper-related genes are upregulated in epithelial cells stimulated with IL-17. STEAP4 functions as a copper reductase and ceruloplasmin (Cp) is the primary carrier of extracellular copper in the body. Lysyl oxidase (LOX) proteins are a class of copper-dependent enzymes that catalyze formation of crosslinks within various types of connective tissues. Source: Li Lab, Department of Immunology, Lerner Research Institute, Cleveland Clinic Foundation.

Thus, the Li Lab sought to investigate a potential copper-dependent mechanism, mediated by STEAP4, that promoted the pro-inflammatory activity of IL-17. Thus, the aims of the experiments presented in this thesis can be described thusly:

Aim 1: Determine whether STEAP4 overexpression and IL-17-signaling promotes copper uptake by colon epithelial cells, and whether induction of inflammation mobilizes copper from latent storage into systemic circulation.

Aim 2: Identify a biochemical mechanism by which IL-17-mediated copper uptake promotes growth in colon epithelial cells.

Aim 3: Determine whether systemic chelation of copper mitigates tumorigenesis in a mouse model of inflammation-associated colorectal cancer.

It was determined that Aim 1 would be investigated through several cell-based experiments. The first experiments would investigate whether STEAP4 overexpression of a colon cancer cell line increased uptake of extracellular copper by the cells compared to cells in which STEAP4 was expressed normally. An additional experiment would seek to determine whether IL-17 stimulation of colon cancer epithelial cells took up more extracellular copper than colon cancer cells which were not stimulated with IL-17.

Finally, a third experiment utilizing a mouse model of colon inflammation would be performed in which animals would be sacrificed throughout the course of the experiment, and the concentration of copper in the liver and the serum would be measured through an atomic absorption method. Aim 2 would be investigated by conducting another cell-based experiment in which activation of growth-promoting signaling pathways would be quantified by Western blot, and this activation would be compared between cells in which STEAP4 was overexpressed and STEAP4 was expressed normally. Finally, Aim 3 would be investigated by utilizing a mouse model of inflammation-associated colorectal cancer, and comparing the number of colon tumors that developed in animals whose body copper levels were left unaltered to animals whose body copper levels were depleted through the administration of a copper chelator by oral gavage.

2.2 Cell Culture

The human colon carcinoma cell line known as LS147T, obtained from the American Type Culture Collection, was used for all cell-based experiments. Cells were grown in high glucose Dulbecco's Modified Eagle Medium, which was supplemented with 10% fetal bovine serum and 2% penicillin-streptomycin. Cell culture dishes were kept in incubators maintained at 37 °C, containing 95% air and 5% CO_2. Prior to harvesting, all cell handling techniques were performed in class 1 biological safety hoods.

2.3 Engineering FLAG-Tagged STEAP4-Inducible LS147T Cells

The STEAP4-inducible cell line was generated by cloning a C-terminal FLAG-tagged STEAP4 cDNA sequence into the pLIX_403 vector. 3 μg of the expression vector was then transfected into HEK-293FT cells using the Lipfectamine2000 reagent, purchased from ThermoFischer, according to the manufacturer's instructions. Medium

from these cells, containing Lentivirus, was then harvested and filtered with 0.45-μM Millex-HP filter 36 hours after the transfection was performed. LS147T cells were then transfected with the Lentivirus using a 1:1 ratio of fresh medium and filter medium containing Lentivirus for 24 hours. Following this, cells were then cultured in fresh medium for 72 hours, and then transfected cells were selected for by growth in medium containing 1 μg/ml puromycin for one week. Finally, cell clones were harvested, and expression of FLAG-tagged STEAP4 was confirmed by Western blot.

2.4 Treatment and Harvesting of Cultured Cells

Before being used in any experiments, cultured cells were grown to around 50% confluence. In the experiments in which the STEAP4-inducible cell line was used, cells receiving doxycycline were treated with 200 ng/mL of the antibiotic 24 hours before any cytokines or copper supplements were added to the medium. Cells used in the copper determination experiments were grown in cell culture dishes with a diameter of 60 mm, and cells used in the cell signaling experiments in which copper was not determined were grown in dishes with a diameter of 35 mm.

In the experiments in which intracellular copper content was measured by atomic absorption spectroscopy, a bulk 100 mM copper sulfate ($CuSO_4$) was prepared with fresh Milli-Q water and was then autoclaved to ensure sterility. Cells treated with copper received the $CuSO_4$ solution by micropipetting such that the final concentration of copper in the medium was 50 μM, not including any copper originally contained therein, at the zero timepoint of the experiment. If cells were treated with both copper and cytokines, the cytokine treatment (50 ng cytokine/mL medium) was administered 24 hours before the copper supplement was added to the medium. The time of copper administration was

defined as the zero timepoint of the experiment. After addition of copper solution or cytokines to the cell medium, the culture dishes were gently swirled for several seconds to distribute the supplements evenly throughout the medium. In the cell signaling experiments not involving copper measurements, cells were treated with cytokine at the zero timepoint, and were then harvested at the timepoints specified in the figures.

Upon harvesting the cells, the medium was removed from the cell dishes by vacuum aspiration. If copper was administered during the experiment, cells were rinsed once with ice cold phosphate buffered saline (PBS) containing 0.1 M ethylenediaminetetraacetic acid (EDTA) to ensure that all extracellular copper was removed, and then once with unaltered, ice cold PBS. If copper was not administered, cells were rinsed twice with unaltered, ice cold PBS. After rinsing, cells were then lifted from the dish with a cell scraper, which was rinsed with PBS and dried with a paper towel in between each use, and then were suspended in PBS. The cell suspension was then transferred to a 15-mL plastic centrifuge tube by pipette. Before centrifugation, the cell suspensions were kept on ice. Cells were then centrifuged for 5 minutes at 3,000 RPM. Following centrifugation, the supernatant was then removed by vacuum aspiration.

In the experiments in which copper was to be determined, cells were lysed using 300 mL of aqueous lysis buffer containing 0.5% Triton X-100, 20 mM HEPES, 150 mM NaCl, 12.5 mM β-glycerophosphate, 1.5mM $MgCl_2$, 10 mM sodium fluoride (NaF), 2 mM dithiothreitol, 1 mM sodium orthovanadate, 2 mM ethylene-bis(oxyethylenenitrilo)tetraacetic acid (EGTA), 20 mM aprotinin and 1 mM phenylmethylsulfonyl fluoride, prepared in Milli-Q water, where the pH was adjusted to

between 7.4 and 7.6. The total protein contents of the raw lysates were then measured by ultraviolet-visible spectrophotometry, using the Bradford protein assay (595 nm), so that the copper content of the samples could be adjusted based on the quantity of cells in each sample. This was accomplished by adding 10 μL of lysate to 1 mL of Bio-Rad Protein Assay Dye Reagent (diluted 5x in Milli-Q water) into a 1-mL cuvette with a pathlength of 1 cm and then pipetting up and down for several seconds to mix the solution. A standard curve was generated using bovine serum albumin (BSA) protein solutions of known concentrations. If any samples registered an absorbance value outside the range of the standard curve, the samples were discarded, and the assay was repeated for all samples by adding a smaller volume of lysate into 1 mL of the protein assay reagent dye until all values were within the range of the curve. After determination of the protein concentrations, 0.7 mL of concentrated nitric acid, purchased from Sigma-Aldrich, were added to the samples (in 1.5-mL microcentrifuge tubes), which were then briefly vortexed and allowed to sit in a 37 °C incubator for 30 minutes to an hour. Samples were then analyzed by atomic absorption spectroscopy (detailed below) after being diluted 10-fold by pipetting 100 μL of acid/lysate homogenate into a fresh 1.5-mL tube containing 900 μL nitric acid. Samples that were not immediately analyzed by AAS were placed in -80 °C storage until the time of analysis.

In the experiments in which intracellular protein contents were to be determined by Western blot, cells were lysed using the same lysis buffer described above. Protein concentrations in each sample were determined by ultraviolet-visible spectroscopy using the method described above, without generating a standard curve. To normalize the protein content of each sample, the most protein-dilute sample was left unaltered, while

all other samples were diluted with lysis buffer based on the ratio of the absorbance T 595 nm of the sample in question to the absorbance at 595 nm of the most dilute sample, such that the final volume of each sample was 1 mL. After the total protein concentrations of the samples were adjusted, each one was mixed with 2x Laemelli sample buffer, supplemented with 100 µL of 2-mercaptoethanol per 900 µL of sample buffer. Samples were then boiled for 5 minutes at 95 °C and kept in -20 °C storage until the time of analysis by Western blot.

2.5 Quantitative Analysis of Proteins by Western Blot

All samples analyzed by Western blot were separated on 10% SDS-PAGE gels prepared using National Diagnostics reagents, which were run at 100 V. The running buffer was a deionized water solution containing 2 M glycine, 0.25 M Tris-HCl, and 0.02 M sodium dodecyl sulfate (SDS). After running the separation gel, protein bands were transferred to a poly(vinylidene difluoride) (or PVDF) membrane pre-soaked in 95% methanol. Each transfer was run for 2 hours at 80 V where the box containing the gel and membrane were kept in an ice bath. The transfer buffer was prepared in deionized water and contained 25 mM Tris-HCl, 200 mM glycine, and 10% methanol. After the transfer, the membrane was blocked with 5% milk solution, dissolved in a wash buffer prepared using deionized water, containing 50 mM Tris-HCl, 150 mM NaCl, and 0.1% Tween-20. After blocking, the membrane was incubated at 4 °C overnight, with gentle shaking, in a primary antibody solution, dissolved in 5% BSA solution prepared in wash buffer. The membrane was then rinsed five times, for five minutes each, in wash buffer, with gentle shaking. Following this, the membranes were then incubated for one hour in the corresponding secondary antibody solution, dissolved in a 5% milk solution prepared

in wash buffer. The membrane was then rinsed again five times, for five minutes each, using wash buffer and gentle shaking. Finally, the membrane was then placed on plastic wrap and then soaked in chemiluminescent Western blot detection reagents obtained from Thermo Fisher for approximately 30 seconds, and then placed in a cassette with autoradiography films and images were obtained using a film developer. The intensity of the protein bands was quantified using ImageJ image processing software.

2.6 Animal Modelling of Colitis and Cancer

Mice were maintained in the Biological Resources Units at Lerner Research Institute of the Cleveland Clinic Foundation. In experiments modelling inflammation only, drinking water in each cage was replaced with an aqueous, 3% dextran sodium sulfate solution for the duration of the experiment to induce colitis [71]. Mice were fed with standard chow and ear tags were used to identify each animal. In mice where both inflammation and colon cancer were modelled, this was achieved by a one-time intraperitoneal injection of azoxymethane (AOM), using 15 mg of the substance per kg of body weight, followed by 3 cycles where drinking water was replaced with a 1.5% DSS solution for 5 days, with two weeks of unaltered drinking water in between each cycle. The first 5-day cycle of DSS solution began on the day of AOM administration. Mice given ammonium tetrathiomolybdate (TTM) were administered treatment of aqueous TTM, using 20 mg per kilogram of body weight, once every three days by oral gavage.

2.7 Animal Sacrifice and Sample Collection

At the time of sacrifice of inflammation-only animals, mice were transported from the BRU to the Li Lab and were administered a 200 μL dose of ketamine through intraperitoneal injection. Immediately after unconsciousness was induced, but while the

animal was still alive, the abdomen was opened with a Y-shaped cut performed with surgical scissors, and a blood sample was collected by cardiac puncture using a 19 G needle attached to a 1-mL syringe. As much blood was collected as possible and was placed in a 1.5-mL microcentrifuge tube after collection. Blood samples were placed on ice immediately after collection and were then centrifuged at 4° C for 15 minutes at 1,000 RPM for 15 minutes. 100 μL of serum was then removed from the microcentrifuge tube by micropipette and was placed in a fresh 1.5-mL tube. The serum was then stored in a -80° C freezer until the time of analysis. Immediately prior to copper analysis, 900 μL of concentrated nitric acid was added to the tube, which was briefly vortexed and then allowed sit in a 37 °C incubator for 30 minutes to 1 hour. After blood collection, a sample of the animal's liver then was removed and placed in a 1.5-mL plastic microcentrifuge tube, which was then placed on dry ice, and later into storage in a -80° C freezer. Immediately before copper analysis, the liver samples were digested in 15-mL centrifuge tubes containing 1 mL concentrated HNO_3 for 30 minutes to 1 hour in a 37 °C incubator. After then being briefly vortexed, 100 μL of liver homogenate was then pipetted into a fresh 1.5-mL microcentrifuge tube containing 900 μL nitric acid to generate the sample that would be tested for copper by atomic absorption.

At the time of sacrifice of colitis-associated carcinoma mice, which was at the conclusion of the third cycle of unaltered drinking water, 8 weeks after AOM injection, animals were brought back to the Li Lab from the BRU and sacrificed by CO_2 asphyxiation. After sacrifice, the abdomen of the animal was opened with a Y-shaped cut and the colon was carefully removed and placed in a dish containing PBS. The colon was then carefully opened longitudinally with scissors and any feces were removed by a

gentle wiping with a PBS-soaked paper towel. Tumor nodules, which were defined as lesions on the colon measuring 1 mm in diameter or greater, were counted visually.

2.8 Determination of Copper by Atomic Absorption

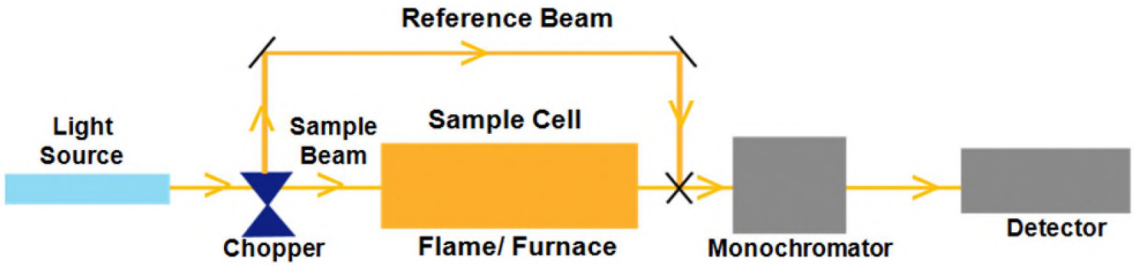

Figure 2.1 — Overview of an atomic absorption spectrometer. A light beam of a specific wavelength is passed through the atomized sample, where the transmittance is compared to the intensity of a reference beam. The wavelength used is specific to the element being analyzed. Source: http://lab-training.com/wp-content/uploads/2013/03/Double-Beam-AAS-Schematic-Diagram.png

All experiments were performed using a Varian FS220 atomic absorption spectrometer from the Case Western Reserve University Department of Chemistry. Samples were analyzed in triplicate using a graphite furnace method. The wavelength used was 324.8 nm with a slit width of 0.5 nm. The following stages of heating were used in the method:

Stage number	Temperature (°C)	Time (s)
1	85	5
2	95	40
3	120	10
4	800	5
5	800	1
6	800	2
7	2300	0
8	2300	2
9	2300	2

Table 2.2 — Stages of heating used in the AAS method. The first three stages are the drying stages, in which water and other volatile solvents present in the solvent are boiled off. Stages four through six are the ashing stages, in which other organic molecules of a higher boiling point are removed from the sample. The final three stages are the analysis stages, in which the element to be analyzed is atomized and analyzed, and then the furnace is heated again to remove any remaining analyte.

Samples were kept under nitrogen gas during analysis and a flow rate of 3 L/min was used. No matrix modifiers were used. The calibration curve was generated using the "automix" feature of the instrument, where the bulk material for standards was a 500 µg/L solution of $CuSO_4$ prepared in concentrated HNO_3, and the makeup material was unaltered concentrated HNO_3.

CHAPTER III

RESUTLS AND DISCUSSION

3.1 STEAP4 Overexpression Increases Copper Uptake by Colon Cancer Cells

A

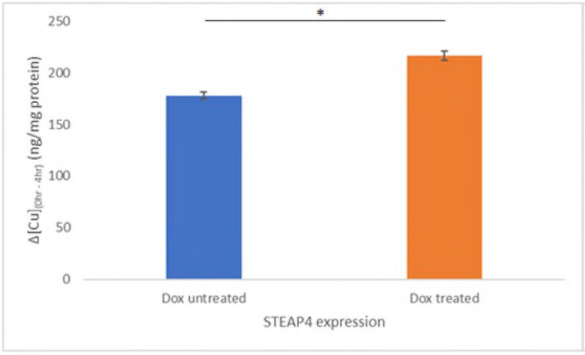

B

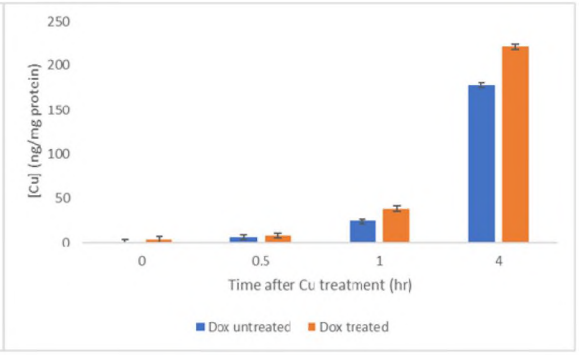

C

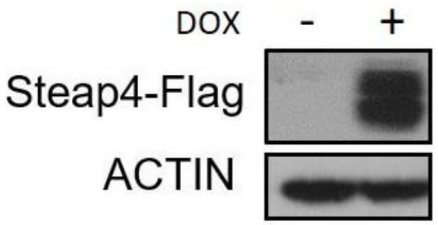

Figure 3.1 — Copper uptake by STEAP4-inducible LS147T cells. Cells were grown to around 50% confluence in 60-mm diameter dishes at the time of doxycycline treatment. A) The change in intracellular copper concentrations over 4 hours in cells treated with doxycycline versus untreated cells. $p = 0.04$. B) intracellular copper concentration measurements at each timepoint in treated and untreated cells. C) Expression of FLAG-tagged STEAP4 in doxycycline-treated cells and untreated cells. All copper measurements were done by GFAAS and each data point was analyzed in triplicate. Error bars represent the standard deviation of each data point.

It has been previously reported [5] that overexpression of STEAP4 in increases the hourly rate of environmental copper uptake in HEK-293T cells, a line derived from human embryonic kidney cells, by approximately 20 percent. And indeed, the data shown in Figure 3.1 indicates from the time of copper treatment (defined as "0 hr") until 4 hours after treatment, STEAP4-overexpressed colon cancer cells take up more extracellular copper from their environment than cells in which STEAP4 is expressed normally. Further, the difference of around 20 percent in the average hourly rates of copper uptake in STEAP4-overexpressed cells compared to cells in which STEAP4 is normally expressed agrees quite well with what has been previously reported. While copper is an essential trace nutrient required by all living systems, it is also true that excess intracellular copper can cause a variety of deleterious biological effects through a chemistry known as the Fenton reaction [72], which occurs via the following scheme:

$$Cu^{+} + H_2O_2 \rightarrow Cu^{2+} + HO\bullet + OH^{-}$$

This immune-mediated production of free radical-containing reactive oxygen species (ROS) through using copper as a redox partner can be used by an organism for host defense purposes, as macrophages are known to release unbound copper ions upon encountering an invading pathogen in a process known as the "respiratory burst" [73]. The primary defensive benefit of this procedure is to cause oxidative damage to a variety of cellular components of the pathogen, particularly its lipids and DNA. For this reason, when stored physiologically, copper must be kept bound to one of many copper-coordinating proteins. Thus, while little data exists to date exploring the potential connection between dietary copper intake and the likelihood of developing various types of cancer – and in fact, surprisingly little is known about the typical amount of copper

consumed by humans who eat modern Western diets, or even the optimum daily intake of the nutrient for adults [11] – it is reasonable to speculate that a higher than normal concentration of body copper, which is partially dependent on STEAP4 expression, may cause an increased risk of tumorigenesis, perhaps due to increased oxidative damage to DNA and subsequent deleterious mutations that copper-mediated Fenton chemistry can cause. It may also be speculated that high body copper levels could potentially lead to increased rate of cancer progression after a tumor has already been established, as copper is required for cell growth generally, as well for angiogenesis [74], the process of creating new blood vessels which provide required nutrients to a growing tumor. Further supporting this idea are previous studies which have reported increased intracellular copper concentrations in a variety of cancers, including colorectal cancer [75]. The full extent of the time scale over which STEAP4 expression affects intracellular copper levels remains unclear, however. Additional investigation into this question is suggested to gain a clearer picture of this connection.

3.2 IL-17 Stimulation Increases Copper Uptake by Colon Cancer Cells

A B

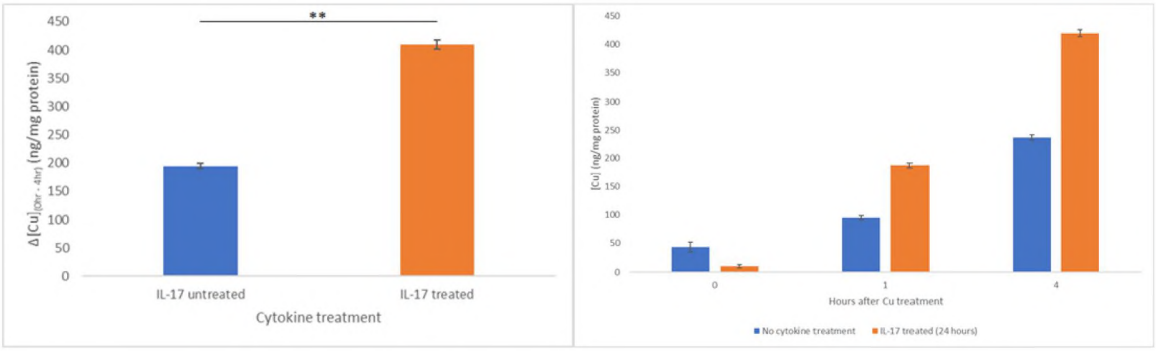

Figure 3.2 — Copper uptake by IL-17-treated and untreated LS147T cells. All samples were analyzed in triplicate by GFAAS. A) The change in intracellular copper concentrations from over 4 hours in cells treated with IL-17 versus untreated cells. p = 0.01. B) Intracellular copper concentration measurements at each timepoint in cytokine-treated and untreated cells. All copper measurements were done by GFAAS and each data point was analyzed in triplicate. Error bars represent the standard deviation of each data point.

Previously published data from the Li Lab has shown that IL-17 stimulation upregulates the expression of STEAP4 in keratinocytes [76]. Further, it has long been known that copper plays a critical role in the regulation of the inflammatory process [77], though the mechanism of this regulation is still not fully understood, outside of the copper-involved respiratory burst mediated by neutrophils, monocytes, and other immune cells. It has also long been known that IL-17 signaling is a critical factor in the progression of colorectal cancer, due to its previously reported pro-inflammatory effects and promotion of a tumor-friendly microenvironment [78]. Previous experiments with inflammation-associated colorectal cancer mice, induced through DSS-AOM treatment, have found that deletion of the IL-17A receptor partially protects against development of colorectal cancer in a genetically-modified mouse model [79]. However, the mechanisms of IL-17's promotion of cancer progression are not yet fully understood. It has been

proposed that these mechanisms may include suppression of the anti-tumor immune response mediated by cytotoxic T cells, promotion of angiogenesis, and activation of the JAK/STAT signaling cascade, which has previously been implicated in the pathogenesis of several different types of cancer [80]. To date, however, the mechanism of IL-17's promotion of tumorigenesis and tumor progression has not been linked directly to a copper-mediated mechanism in the literature. Data presented in this thesis suggest that this previously proposed promotion of angiogenesis by IL-17 may be driven by its upregulation of STEAP4, and the resulting increase in the copper levels of tumor cells.

Though IL-17-producing CD4+ T cells (also known as Th17 cells) were originally thought of as the only significant producers of IL-17, evidence has since emerged that many different types of immune cells are capable of producing the cytokine as well, particularly innate immune cells such as natural killer (NK) cells and neutrophils [81]. Interestingly, it has also been reported that a highly specialized type of epithelial cell found in the intestinal crypts known as Paneth cells are capable of rapidly producing IL-17 (and other pro-inflammatory mediators) upon exposure to inflammatory cytokine signals [82]. Enterocytes, the epithelial cells that line the lumen of the small intestine, are the primary cells responsible for the uptake of dietary copper, after its reduction from the cupric state to the cuprous state [83]. Thus, taking the data from Figure 3.2 into account, it can be reasonably inferred that the presence of inflammation in the gut, which directly causes the sustained release of IL-17 by Paneth cells, likely stimulates increased uptake of dietary copper *in vivo,* and thus creates a positive feedback loop which sustains the local inflammatory response, thereby creating a tumor-promoting microenvironment.

One additional implication of the crucial role that copper metabolism plays in the progression of cancer is its relevance to platinum-containing anti-cancer drugs. A mainstay of frontline treatments for many types of cancer, including colorectal cancer, platinum therapies such as cisplatin (often referred to as the "penicillin of cancer"), as well as oxaliplatin, commonly prescribed to colorectal cancer patients, are known to cause cell death by mediating DNA damage through a mechanism of generating both intrastrand and interstrand crosslinking via platinum adducts, which in turn induces apoptosis [84]. As these platinum-containing drugs are taken up into the cells by copper transport proteins including ATP7A, ATP7B, and most notably CTR1, they affect rapidly dividing cells most strongly, and thus can effectively target malignant cells while minimizing damage to healthy tissues [85]. However, with the exception of germ cell tumors, acquired resistance to these drugs is a virtually unavoidable result of platinum therapy [86]. It is possible that treatment with copper chelators may be able to mitigate this problem, however, as it has been reported that the uptake of platinum-based drugs by tumor cells can be enhanced through treatment with ammonium tetrathiomolybdate [87]. While further study into this route of treatment is required to better elucidate its effectiveness, it is suggested that copper chelation by TTM may incur the dual benefits of reducing the tumor-promoting effects of copper uptake via promotion of angiogenesis and stimulation of cell growth and proliferation, and also by re-sensitizing tumor cells to DNA damage caused by platinum therapy, by upregulating the expression of copper uptake membrane proteins such as CTR1 that are responsible for platinum uptake into the cell.

3.3 Colitis Mobilizes Copper from Latent Storage in the Liver into Systemic Circulation

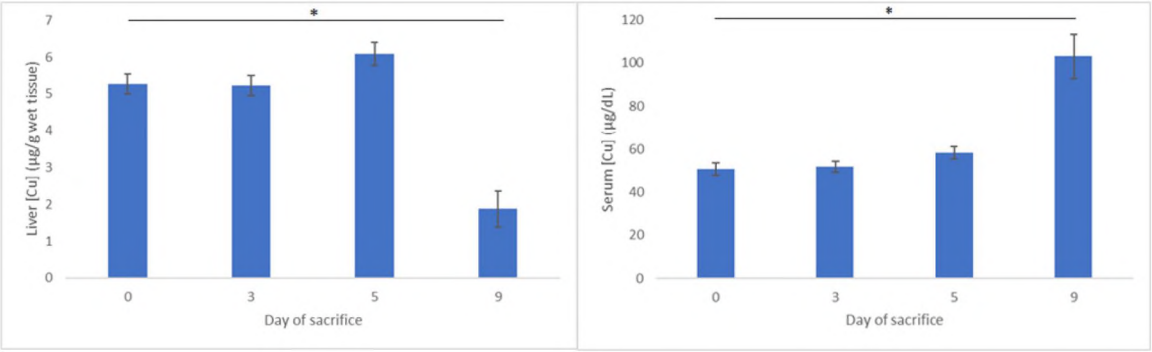

Figure 3.3 — Colitis induces mobilization of latent copper stored in the liver into systemic circulation. First panel: liver concentrations of intracellular copper in mice over the course of DSS treatment. $p = 0.04$. Second panel: serum copper concentrations mice over the course of DSS treatment. $p = 0.05$. Day 0 represents the time at which the animals' drinking water was replaced by an aqueous 3% DSS solution. P-values reflect a comparison between copper concentrations measured on day 0 and copper concentrations measured on day 9. All copper measurements were done by GFAAS and each animal's sample was analyzed in triplicate. Error bars represent the standard deviation of each data point. $n = 3$.

As has been mentioned previously, the liver is the largest storage site of copper in the body [2]. While this has long been known, and it has also long been known that the liver is a common site of colorectal cancer metastases, it has been believed that this is primarily due to the high volume of blood flow from the intestines to the liver via the hepatic portal vein, which provides a route of transportation of malignant cells from the intestines to the liver. And while this is likely correct, it is suggested that the abundance of copper may play a role in the success of intestinal cancer metastases in the liver as well.

Upon reduction by a STEAP protein and uptake across the apical membrane into an enterocyte by CTR1, the copper ion is immediately bound to one of several copper chaperone proteins to prevent unwanted redox reactions from occurring within the cell.

From there, depending on which protein the ion binds to, it is shuttled to one of several locations – binding to COX17 delivers copper to the mitochondria, where it is incorporated into cytochrome c oxidase, which is a crucial protein involved in cellular respiration [88]. It may also be shuttled to the trans-Golgi network by ATOX1, where it can be exported to the bloodstream by ATP7A or ATP7B, and then on to another destination within the body [89]. A third important destination of the copper ions is the cytosol of the enterocyte that initially took them up, where it can be shuttled by CCS to superoxide dismutase (SOD1), a critical protein which converts intracellular superoxide radicals (O_2^-) into molecular oxygen, and thus prevents unwanted radical-generating reactions from occurring within the cell [90]. Excess intracellular copper may also be bound to metallothionein. If the ion is exported to the bloodstream, it binds to α_2-macroglobulin or albumin and is taken up into a hepatocyte by CTR1. From there, it can be transported to mitochondria or superoxide dismutase within the hepatocyte, or shuttled to the trans-Golgi network and exported again to the bloodstream, where it binds to ceruloplasmin or albumin, and is then distributed to cells and tissues around the body [91].

It has been reported previously that elevated serum copper in mouse models of breast and lung cancer occur concomitantly with a decrease in liver copper levels [92]. The data shown in Figure 3.3 indicate that this is the case in a mouse model of inflammatory bowel disease as well. Copper, therefore, is being mobilized from the site of storage into systemic blood circulation, which likely increases the risk of tumorigenesis directly via the increased risk of oxidative DNA damage through Fenton reaction-mediated production of reactive oxygen species at the site of inflammation, as

well as indirectly by sustaining the chronic inflammatory response and resulting tumor-promoting environment at the site of inflammation. This also likely sustains tumor progression as well by providing the copper necessary for continued cell growth and angiogenesis. Therefore, it is suggested that copper depletion therapy may simultaneously serve the dual functions of slowing the progression of a primary colon tumor by depriving it of the resources necessary for growth, and may additionally decrease the likelihood of a secondary tumor successfully establishing in the liver as well due to less copper being available in the local environment

3.4 STEAP4 Overexpression Enhances IL-17-Mediated Activation of Growth Pathways in Colon Cancer Cells

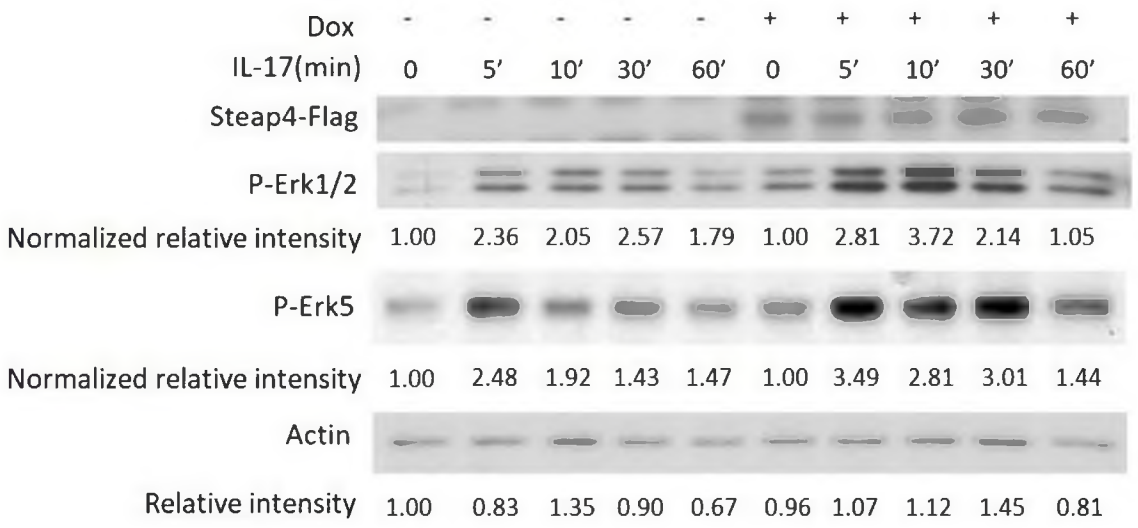

Figure 3.4 — STEAP4 overexpression enhances IL-17-mediated activation of MAPK/ERK signaling in LS147T cells. Activation of ERK1/2 and ERK5 is increased in doxycycline-treated cells compared to untreated cells. The relative intensity of each band was quantified using ImageJ software. The intensities of the p-ERK1/2 and p-ERK5 bands from the zero timepoint from the treated cell group and the untreated cell group were defined as 1 for each respective group. "Normalized relative intensity" was obtained by dividing the intensity of each band by the intensity of the band from the zero timepoint from its group, after the intensity value for each band had been normalized against the intensity of its corresponding actin band.

Colorectal carcinogenesis is a complex biological event involving dysregulation of the growth, proliferation, and differentiation of enterocytes, as well as of pro-apoptotic and cell survival mechanisms [93]. These cell cycle processes are regulated by a variety of internal as well as external signals. External signals perform this regulation by binding to cell membrane receptors and thus triggering the corresponding signaling cascade. One significant example of these externally regulated signaling pathways is the mitogen-activated protein kinase/extracellular signal regulated-kinase, or MAPK/ERK pathway. Being members of the serine-threonine kinase family, it has long been known that this pathway is critical regulator of human gene expression and cellular proliferation [94]. Accordingly, the MAPK/ERK signaling cascade has previously been implicated in several different types of cancers [95]. The ERK signaling pathway specifically, of three known pathways falling under the MAPK family, is communicated through the activation of Protein Kinase C, or PKC. PKC in turn activates RAF1, which then activates MEK. MEK then activates ERK, which can then directly phosphorylate various transcription factors, which themselves directly affect gene expression related to proliferation and cell survival [96].

IL-17 signaling is known to activate several important cell growth and proliferation pathways, including the PI3K-AKT and NF-κB pathways, in addition to the ERK signaling cascade [97]. The data presented in Figure 3.4 demonstrates that this activation of ERK signaling is enhanced by overexpression of STEAP4, suggesting that copper plays an important role in this process. A previous report demonstrated that deletion or mutation of copper transporter 1 (CTR1), as well as treatment with a copper chelator, can inhibit this signaling pathway by reducing the ability of MEK1 to

phosphorylate ERK [98], further substantiating this assertion. It is therefore suggested that inhibiting IL-17 signaling and administering copper depletion therapy concurrently could be more effective in retarding tumor progression than either treatment separately, though further investigation into this assertion is recommended.

3.5 Copper Chelation as Potential Anti-Cancer Therapy and Future Directions

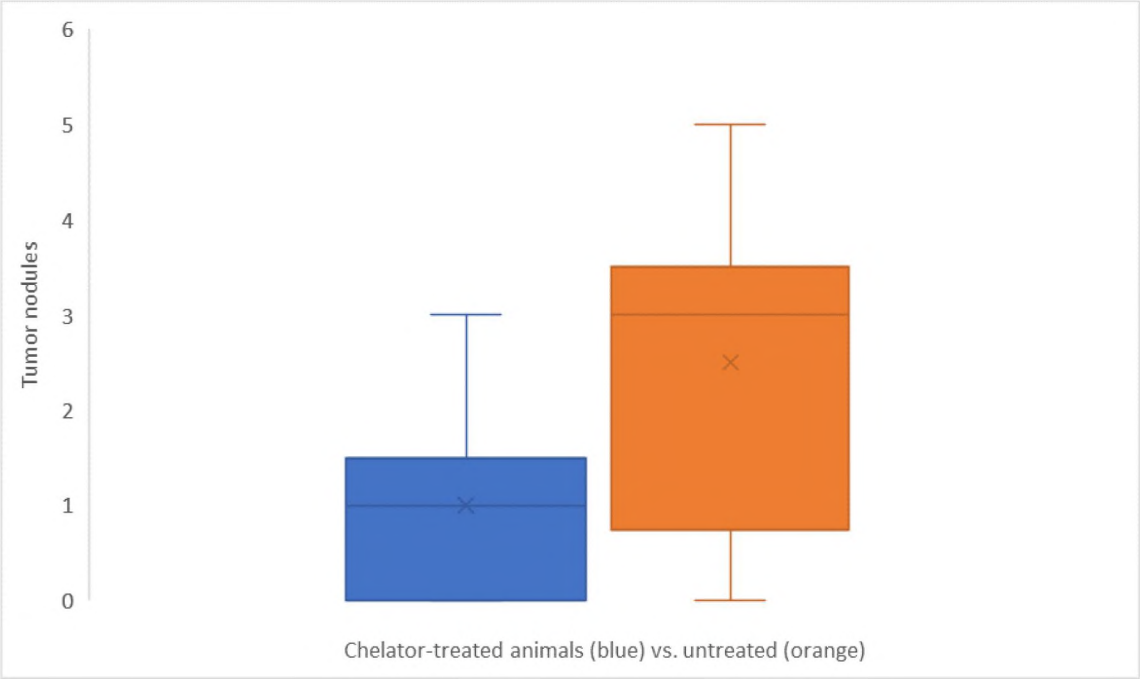

Figure 3.5 — Copper chelation potentially decreases the number of tumor nodules in DSS-AOM mice. Animals were sacrificed by CO_2 asphyxiation at the conclusion of the third "recovery cycle" of unaltered drinking water, 8 weeks after AOM injection and the beginning of the first DSS-treated drinking water cycle. Tumor nodules were identified by visual inspection and were defined as any lesion on the colon measuring 1 mm in diameter or larger. The "x" from each box signifies the median value for the group and the line signifies the mean. $n = 6$. $p = 0.16$.

Given all of the data shown thus far, the practical question to ask is whether copper depletion could be an effective treatment for inflammation-associated colorectal cancer patients. Ammonium tetrathiomolybdate (TTM) is a copper chelator that is used to treat Wilson's Disease, a condition characterized by a defect in ATP7B that causes excess copper accumulation in the liver and brain [99]. While TTM is currently only

approved by the Food and Drug Administration for treatment of Wilson's Disease (administered orally in the form of capsule), it has very recently been reported that TTM treatment inhibits inflammatory responses in microglia cells *in vitro* [100]. The molecule is also currently being investigated as a therapy for breast cancer [101]. While the data displayed in Figure 3.6 did not find a statistically significant difference in the development of tumor nodules between the animals treated with the chelator and the animals gavaged only with water, they do suggest that further study into whether or not TTM is an effective treatment for colorectal cancer patients could be valuable.

While colorectal cancer can usually be treated relatively easily when detected early, effective treatment of metastatic colon cancer remains a significant clinical challenge with few good therapeutic options. While the five-year survival rate for patients diagnosed with stage 1 through stage 3 colorectal cancer ranges from 92% to 53%, the rate for patients diagnosed with stage 4 of the disease stands at a dismal 11% [102]. There is, therefore, an urgent need to find effective treatments for patients diagnosed with metastatic colorectal cancer. As was mentioned earlier, the liver is the most common site of metastasis for primary colon tumors, and is also the largest site of copper storage in the body. Previous studies have reported that in mice which were genetically programmed to develop breast cancer, copper depletion treatment did not prevent the formation of tumors in the breast tissue, but animals treated with TTM developed tumors that were too small to be observed visually, while untreated animals developed easily visible tumors [103]. Therefore, it is recommended that additional studies be performed to investigate the potential of copper depletion therapy to prevent the growth of additional tumors after the initial one is discovered. It is likely that further

investigation into this route of cancer treatment, in patients afflicted with colorectal and other cancers will continue into the future.

3.6 Statistical Analysis

Pipette volumes were assumed to have a standard deviation of ±2%.

Tissue samples were massed to two decimal points of accuracy.

Statistical Calculations for Figure 3.1

Error in AAS measurements

$$\Delta[\mathrm{Cu}] = [\mathrm{Cu}]_{4\ hr} - [\mathrm{Cu}]_{0\ hr}$$

$$\Delta[\mathrm{Cu}]_{treated} = 220.4820171 - 3.762017139 = 216.719999961\ \frac{\mathrm{ng}}{\mathrm{mg\ protein}}$$

$$\Delta[\mathrm{Cu}]_{untreated} = 177.8407422 - 0.073274351 = 177.767467849\ \frac{\mathrm{ng}}{\mathrm{mg\ protein}}$$

$$\sigma_{\Delta[\mathrm{Cu}],absorbance} = \sqrt{\sigma_{[\mathrm{Cu}],0\ hr}{}^2 + \sigma_{[\mathrm{Cu}],4\ hr}{}^2}$$

$$\sigma_{\Delta\,[\mathrm{Cu}],treated} = \sqrt{\sigma_{\,[\mathrm{Cu}],treated,0\ hr}{}^2 + \sigma_{\,[\mathrm{Cu}],treated,4\ hr}{}^2}$$

$$\sigma_{\Delta[\mathrm{Cu}],treated} = \sqrt{(\frac{0.086248476}{3})^2 + (\frac{0.096754824}{3})^2} = 0.04320531806206$$

$$\sigma_{\Delta[\mathrm{Cu}],untreated} = \sqrt{\sigma_{[\mathrm{Cu}],untreated,0\ hr}{}^2 + \sigma_{\,[\mathrm{Cu}],untreated,4\ hr}{}^2}$$

$$\sigma_{\Delta[\mathrm{Cu}],untreated} = \sqrt{(\frac{0.081990144}{3})^2 + (\frac{0.103151556}{3})^2} = 0.043922440756864$$

$$\sigma_{\Delta[\mathrm{Cu}],total} = \sqrt{\sigma_{\Delta\mathrm{Cu},treated}{}^2 + \sigma_{\Delta\mathrm{Cu},untreated}{}^2}$$

$$\sigma_{\Delta[\mathrm{Cu}],total} = \sqrt{0.04320531806206^2 + 0.043922440756864^2}$$

$$\sigma_{\Delta[\mathrm{Cu},]total} = 0.061610715877061$$

$$\sigma_{\Delta\mathrm{Cu},absorbance} = 0.061610715877061$$

Error in sample volumes

$$\sigma_{volume} = \sqrt{\left(\frac{[\mathrm{Cu}]_{treated,0hr}}{\mathrm{vol}+\sigma} - \frac{[\mathrm{Cu}]_{treated,0hr}}{\mathrm{vol}}\right)^2 + \left(\frac{[\mathrm{Cu}]_{treated,4hr}}{\mathrm{vol}+\sigma} - \frac{[\mathrm{Cu}]_{treated,4hr}}{\mathrm{vol}}\right)^2 + \left(\frac{[\mathrm{Cu}]_{untreated,0hr}}{\mathrm{vol}+\sigma} - \frac{[\mathrm{Cu}]_{untreated,0hr}}{\mathrm{vol}}\right)^2 + \left(\frac{[\mathrm{Cu}]_{untreated,4hr}}{\mathrm{vol}+\sigma} - \frac{[\mathrm{Cu}]_{untreated,4hr}}{\mathrm{vol}}\right)^2}$$

$$\sigma_{volume} = \sqrt{\left(\frac{3.762017139}{1.02} - \frac{3.762017139}{1}\right)^2 + \left(\frac{220.4820171}{1.02} - \frac{220.4820171}{1}\right)^2 + \left(\frac{0.073274351}{1.02} - \frac{0.073274351}{1}\right)^2 + \left(\frac{177.8407422}{1.02} - \frac{177.8407422}{1}\right)^2}$$

$$\sigma_{volume} = 5.6658110888888$$

Total error

$$\sigma_{total} = \sqrt{{\sigma_{absorbace}}^2 + {\sigma_{volume}}^2}$$

$$\sigma_{total} = \sqrt{0.061610715877061^2 + 5.6658110888888^2}$$

$$\sigma_{total} = 5.6661460601794$$

$$\mathrm{t} = \frac{\Delta[\mathrm{Cu}]_{treated} - \Delta[\mathrm{Cu}]_{untreated}}{\sigma_{total}}$$

$$\mathrm{t} = \frac{216.719999961 - 177.8407422}{5.6661460601794}$$

$$\mathrm{t} = 6.86167588129$$

$$\mathrm{p} = 0.04$$

Statistical Calculations for Figure 3.2

Error in AAS measurements

$$\Delta[\mathrm{Cu}]_{treated} = 419.7013339 - 10.62239755 = 409.07893635 \frac{\mathrm{ng}}{\mathrm{mg\ protein}}$$

$$\Delta[\mathrm{Cu}]_{untreated} = 237.0232717 - 42.67507704 = 194.34819466\ \frac{\mathrm{ng}}{\mathrm{mg\ protein}}$$

$$\sigma_{\Delta[\mathrm{Cu}],absorbance} = \sqrt{\sigma[\mathrm{Cu}]_{0\ hr}{}^2 + \sigma[\mathrm{Cu}]_{4\ hr}{}^2}$$

$$\sigma_{\Delta\ [\mathrm{Cu}],treated} = \sqrt{(\frac{0.0768144}{3})^2 + (\frac{0.971792}{3})^2} = 0.325000858261$$

$$\sigma_{\Delta\ [\mathrm{Cu}],untreated} = \sqrt{(\frac{0.0424896}{3})^2 + (\frac{0.7554624}{3})^2} = 0.25221877715$$

$$\sigma_{\Delta[\mathrm{Cu}],total} = \sqrt{\sigma_{\Delta[\mathrm{Cu}],treated}{}^2 + \sigma_{\Delta[\mathrm{Cu}],untreated}{}^2}$$

$$\sigma_{\Delta[\mathrm{Cu}],total} = \sqrt{0.325000858261^2 + 0.25221877715^2}$$

$$\sigma_{\Delta[\mathrm{Cu}],total} = 0.411387736105\ \frac{\mathrm{ng}}{\mathrm{mg\ protein}}$$

Error in sample volumes

Sample volume = 300 µL lysate + 700 µL acid = 1 mL

Sample volume SD = 6 µL lysate + 14 µL acid = 20 µL

$$\sigma_{volume} = \sqrt{\begin{array}{l}(\frac{[\mathrm{Cu}]_{treated,0hr}}{\mathrm{vol} + \sigma} - \frac{[\mathrm{Cu}]_{treated,0hr}}{\mathrm{vol}})^2 + ([\frac{[\mathrm{Cu}]_{treated,4hr}}{\mathrm{vol} + \sigma} - \frac{[\mathrm{Cu}]_{treated,4hr}}{\mathrm{vol}})^2 + \\ (\frac{[\mathrm{Cu}]_{untreated,0hr}}{\mathrm{vol} + \sigma} - \frac{[\mathrm{Cu}]_{untreated,0hr}}{\mathrm{vol}})^2 + (\frac{[\mathrm{Cu}]_{untreated,4hr}}{\mathrm{vol} + \sigma} - \frac{[\mathrm{Cu}]_{untreated,4hr}}{\mathrm{vol}})^2\end{array}}$$

$$\sigma_{volume} = \sqrt{\begin{array}{l}(\frac{10.62239755}{1.02} - \frac{10.62239755}{1})^2 + (\frac{419.7013339}{1.02} - \frac{419.7013339}{1})^2 + (\frac{42.67507704}{1.02} \\ - \frac{42.67507704}{1})^2 + (\frac{237.0232717}{1.02} - \frac{237.0232717}{1})^2\end{array}}$$

$$\sigma_{volume} = 9.4903427013242$$

Total error

$$\sigma_{total} = \sqrt{\sigma_{absorbace}{}^2 + \sigma_{volume}{}^2}$$

$$\sigma_{total} = \sqrt{0.411387736105^2 + 9.4903427013242^2}$$

$$\sigma_{total} = 9.4992549422571$$

$$t = \frac{\Delta[Cu]_{treated} - \Delta[Cu]_{untreated}}{\sigma_{total}}$$

$$t = \frac{409.07893635 - 194.34819466}{9.4992549422571}$$

$$t = 22.5263157895$$

$$p = 0.01$$

Statistical Calculations for Figure 3.3 (A)

Error in AAS measurements

$$\sigma_{[Cu,individual\ timepoints]} = \sqrt{\sigma_{[Cu],Day\ 0,point1}{}^2 + \sigma_{[Cu],Day\ 9,point2}{}^2 + \sigma_{[Cu],Day\ 9,point1}{}^2 + \sigma_{[Cu],Day\ 9,point2}{}^2 + \sigma_{[Cu],Day\ 9,point3}{}^2}$$

$$\sigma_{[Cu,individual\ timepoints]} = \sqrt{(\frac{6.73x10^{-5}}{3})^2 + (\frac{6.7x10^{-5}}{3})^2 + (\frac{3.42x10^{-6}}{3})^2 + (\frac{5.6x10^{-6}}{3})^2 + (\frac{3.8x10^{-5}}{3})^2}$$

$$\sigma_{[Cu,individual\ timepoints]} = 0.0000341651973668$$

$$\sigma_{[Cu,absorbance,cumulative\ timepoints]} = \sqrt{\sigma_{[Cu],Day\ 0}{}^2 + \sigma_{[Cu],Day\ 9}{}^2}$$

$$\sigma_{[Cu,cumulative\ timepoints]} = \sqrt{(\frac{0.385}{2})^2 + (\frac{1.199834}{3})^2}$$

$$\sigma_{[Cu,cumulative\ timepoints]} = 0.4438660323069$$

$$\sigma_{[\mathrm{Cu},total]} = \sqrt{\sigma_{[\mathrm{Cu}],individual\ timepoints}{}^2 + \sigma_{[\mathrm{Cu},]cumulative\ timepoints}{}^2}$$

$$\sigma_{[\mathrm{Cu},total]} = \sqrt{0.0000341651973668^2 + 0.44386603230692}$$

$$\sigma_{[\mathrm{Cu}],total} = 0.443866033622$$

$$\sigma_{[\mathrm{Cu}],absorbance} = 0.443866033622$$

Error in sample volumes

Sample volume = 100 µL liver homogenate + 900 acid = 1 mL

Sample volume SD = 2 uL + 18 uL = 20 uL

$$\sigma_{volume} = \sqrt{\begin{array}{c}(\frac{[\mathrm{Cu}]_{Day\ 0,point1}}{\mathrm{vol} + \sigma} - \frac{[\mathrm{Cu}]_{Day\ 0,point1}}{\mathrm{vol}})^2 + (\frac{[\mathrm{Cu}]_{Day\ 0,point2}}{\mathrm{vol} + \sigma} - \frac{[\mathrm{Cu}]_{Day\ 0,point2}}{\mathrm{vol}})^2 \\ +(\frac{[\mathrm{Cu}]_{Day\ 9,point1}}{\mathrm{vol} + \sigma} - \frac{[\mathrm{Cu}]_{Day\ 9,point1}}{\mathrm{vol}})^2 + (\frac{[\mathrm{Cu}]_{Day\ 9,point2}}{\mathrm{vol} + \sigma} \\ -\frac{[\mathrm{Cu}]_{Day\ 9,point2}}{\mathrm{vol}})^2 + (\frac{[\mathrm{Cu}]_{Day\ 9,point3}}{\mathrm{vol} + \sigma} - \frac{[\mathrm{Cu}]_{Day\ 9,point3}}{\mathrm{vol}})^2\end{array}}$$

$$\sigma_{volume} = \sqrt{\begin{array}{c}(\frac{4.8895}{1.02} - \frac{4.8895}{1})^2 + (\frac{5.6595}{1.02} - \frac{5.6595}{1})^2 + (\frac{3.5651}{1.02} - \frac{3.5651}{1})^2 \\ + (\frac{1.1088}{1.02} - \frac{1.1088}{1})^2 + (\frac{0.9394}{1.02} - \frac{0.9394}{1})^2\end{array}}$$

$$\sigma_{volume} = 0.16823673595265$$

Error in measurement of liver tissue mass

$$\text{Mean tissue samples mass} = \frac{0.53 + 0.46 + 0.57 + 0.49 + 0.52}{5}$$

Mean tissue sample mass = 0.514 g

Balance error = ± 0.005 g

$$\text{Average \% error in tissue mass measurement} = \frac{0.01}{0.514}$$

Average % error in tissue mass measurement = 0.01945525291

$$\sigma_{volume+mass} = \sigma_{volume}\ x\ 1.01945525291$$

$$\sigma_{volume+mass} = 0.16823673595265\ x\ 1.01945525291$$

$$\sigma_{volume+mass} = 0.17150982419$$

Total error

$$\sigma_{total} = \sqrt{\sigma_{absorbace}{}^2 + \sigma_{volume+mass}{}^2}$$

$$\sigma_{total} = \sqrt{0.443866033622^2 + 0.17150982419^2}$$

$$\sigma_{total} = 0.47584942534063$$

$$t = \frac{(5.2745 - 1.8711)}{0.47584942534063}$$

$$t = 7.15226249893$$

$$p = 0.04$$

Statistical Calculations for Figure 3.3 (B)

Error in AAS measurements

$$\sigma_{[Cu,individual\ timepoints]} = \sqrt{\sigma_{[Cu],Day\ 0,point1}{}^2 + \sigma_{[Cu],Day\ 9,point2}{}^2 + \sigma_{[Cu],Day\ 9,point1}{}^2 + \sigma_{[Cu],Day\ 9,point2}{}^2 + \sigma_{[Cu],Day\ 9,point3}{}^2}$$

$$\sigma_{[Cu,individual\ timepoints]} = \sqrt{(\frac{1.767745}{3})^2 + (\frac{0.062935}{3})^2 + (\frac{0.13995}{3})^2 + (\frac{0.145203}{3})^2 + (\frac{0.132101}{3})^2}$$

$$\sigma_{[Cu,individual\ timepoints]} = 0.595097445145$$

$$\sigma_{[Cu,cumulative\ timepoints]} = \sqrt{\sigma_{[Cu],Day\ 0}{}^2 + \sigma_{[Cu],Day\ 9}{}^2}$$

$$\sigma_{[Cu,cumulative\ timepoints]} = \sqrt{(\frac{2.17865}{2})^2 + (\frac{10.60767}{3})^2}$$

$$\sigma_{[\mathrm{Cu},cumulative\ timepoints]} = 3.69988473438$$

$$\sigma_{[\mathrm{Cu},total]} = \sqrt{\sigma_{[\mathrm{Cu}],individual\ timepoints}{}^2 + \sigma_{[\mathrm{Cu}],cumulative\ timepoints}{}^2}$$

$$\sigma_{[\mathrm{Cu},total]} = \sqrt{0.595097445145^2 + 3.69988473438^2}$$

$$\sigma_{[\mathrm{Cu}],absorbance,total} = 3.74743752675$$

Error in sample volumes

$$\text{Sample volume} = 100\ \mu\text{L serum} + 900\ \mu\text{L acid} = 1\ \text{mL}$$

$$\text{Sample volume SD} = 6\ \mu\text{L lysate} + 14\ \mu\text{L acid} = 20\ \mu\text{L}$$

$$\sigma_{volume} = \sqrt{\begin{array}{c}(\frac{[\mathrm{Cu}]_{Day\ 0,point1}}{\mathrm{vol} + \sigma} - \frac{[\mathrm{Cu}]_{Day\ 0,point1}}{\mathrm{vol}})^2 + (\frac{[\mathrm{Cu}]_{Day\ 0,point2}}{\mathrm{vol} + \sigma} - \\ \frac{[\mathrm{Cu}]_{Day\ 0,point2}}{\mathrm{vol}})^2 + (\frac{[\mathrm{Cu}]_{Day\ 9,point1}}{\mathrm{vol} + \sigma} - \frac{[\mathrm{Cu}]_{Day\ 9,point1}}{\mathrm{vol}})^2 + \\ -(\frac{[\mathrm{Cu}]_{Day\ 9,point2}}{\mathrm{vol} + \sigma} - \frac{[\mathrm{Cu}]_{Day\ 9,point2}}{\mathrm{vol}})^2 + (\frac{[\mathrm{Cu}]_{Day\ 9,point3}}{\mathrm{vol} + \sigma} - \frac{[\mathrm{Cu}]_{Day\ 9,point3}}{\mathrm{vol}})^2\end{array}}$$

$$\sigma_{volume} = \sqrt{\begin{array}{c}(\frac{52.7685}{1.02} - \frac{52.7685}{1})^2 + (\frac{48.4112}{1.02} - \frac{48.4112}{1})^2 + (\frac{116.625}{1.02} - \frac{116.625}{1})^2 \\ +(\frac{90.752}{1.02} - \frac{90.752}{1})^2 + (\frac{101.6165}{1.02} - \frac{101.6165}{1})^2\end{array}}$$

$$\sigma_{volume} = 3.8621956490546$$

Total error

$$\sigma_{total} = \sqrt{\sigma_{absorbace}{}^2 + \sigma_{volume}{}^2}$$

$$\sigma_{total} = \sqrt{3.74743752675^2 + 3.8621956490546^{\,2}}$$

$$\sigma_{total} = 9.4992549422571$$

$$\mathrm{t} = \frac{(102.9978333 - 50.58985)}{9.4992549422571}$$

$$\mathrm{t} = 5.51706250844$$

$$p = 0.05$$

Statistical Calculations for Figure 3.5

$$\text{Avg \# of tumor nodules}_{treated} = 1$$

$$\text{Avg \# of tumor nodules}_{untreated} = 2.5$$

$$\sigma_{treated} = 1.095445$$

$$\sigma_{untreated} = 1.760682$$

$$\sigma_{total} = \sqrt{{\sigma_{treated}}^2 + {\sigma_{untreated}}^2}$$

$$\sigma_{total} = \sqrt{1.095445^2 + 1.760682^2}$$

$$\sigma_{total} = 2.07354434105$$

$$t = \frac{(2.5 - 1)}{(\frac{2.07364434105}{\sqrt{6}})}$$

$$t = 1.77187309388$$

$$p = 0.16$$

CHAPTER IV

CONCLUSION

Despite encouraging progress that has been made, colorectal cancer remains a significant clinical challenge. This is particularly true in patients who do not regularly receive colonoscopies, as the disease becomes significantly more difficult to treat effectively in its later stages. Despite the American Cancer Society's recommendation that adults aged 45 years or older get screened for colorectal cancer, fully one-third of adults 50 to 75 years of age have never received a colonoscopy [104]. For this reason, a better understanding of the pathogenesis of colorectal cancer and new treatment options, particularly for metastatic tumors, is urgently needed.

It has long been known that chronic inflammation increases an individual's risk of developing colorectal cancer [32]. While inflammation is a remarkably complex biological response, it is known that interleukin 17 is a critical mediator of the inflammatory process. Thus, IL-17 is a promising target for anti-cancer therapies that has been investigated for many years now [78]. The precise role that IL-17, and inflammation generally plays in tumorigenesis and tumor progression is still not fully understood. Data presented in this thesis suggest that the pro-inflammatory and the cancer-promoting properties of IL-17 are dependent, at least in part, on copper.

A

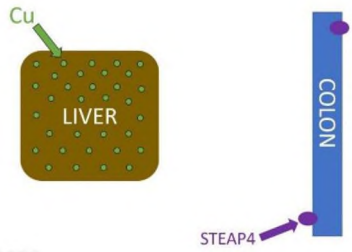
Cu
LIVER
COLON
STEAP4

C

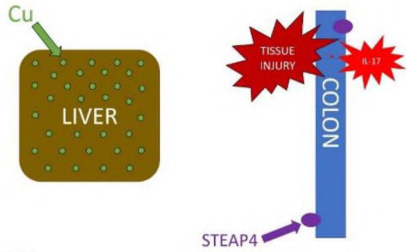
Cu
LIVER
TISSUE INJURY
IL-17
COLON
STEAP4

E

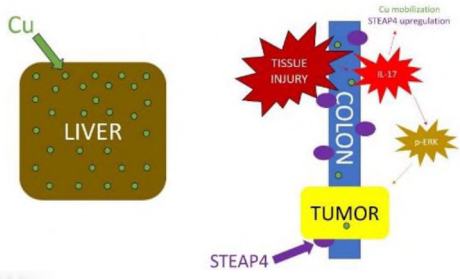
Cu
LIVER
Cu mobilization
STEAP4 upregulation
TISSUE INJURY
IL-17
COLON
p-ERK
TUMOR
STEAP4

B

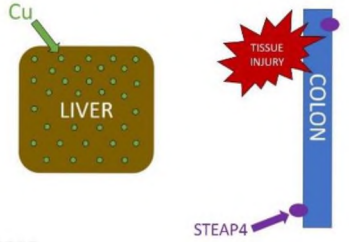
Cu
LIVER
TISSUE INJURY
COLON
STEAP4

D

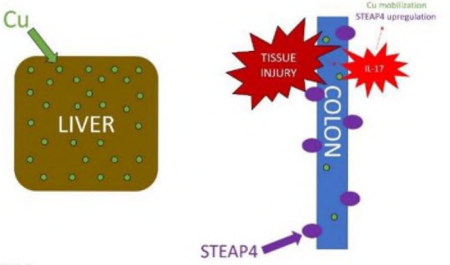
Cu
LIVER
Cu mobilization
STEAP4 upregulation
TISSUE INJURY
IL-17
COLON
STEAP4

F

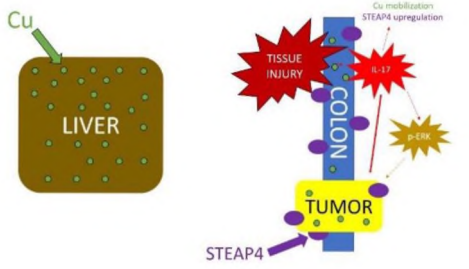
Cu
LIVER
Cu mobilization
STEAP4 upregulation
TISSUE INJURY
IL-17
COLON
p-ERK
TUMOR
STEAP4

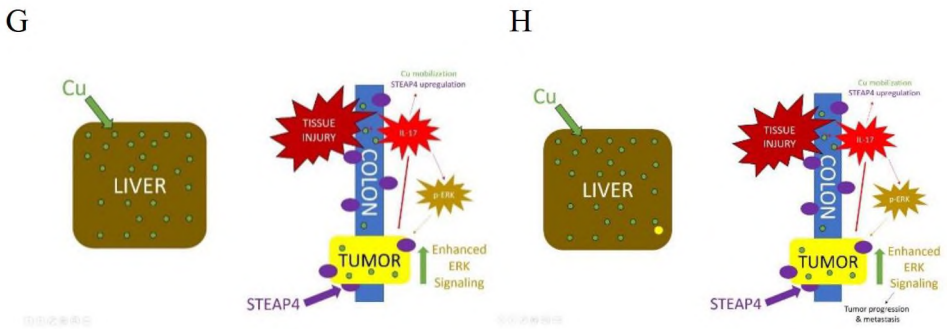

Figure 4.1 – A proposed visual model of IL-17's effects on copper mobilization and tumor promotion. The colon is represented in blue, the liver is represented in brown, STEAP4 is represented in purple, and copper ions are represented in green. A) The liver and colon are healthy and normal, and STEAP4 is expressed normally in colon epithelial cells. B) The colon epithelium suffers and injury (represented in red). C) The injury to the colon tissue causes Paneth cells and white blood cells from the local blood supply to begin secreting IL-17 (represented in crimson). D) IL-17-mediated inflammation causes latent copper stored in the liver to be mobilized into systemic circulation. IL-17 stimulation additionally induces increased expression of STEAP4 by colon epithelial cells. This overexpression of STEAP4 causes colon epithelial cells to increase the amount of copper they take up from the blood. E) IL-17 signaling causes increased ERK signaling (represented in gold) in colon epithelial cells, promoting cell survival and increasing cell growth and proliferation, and thus the risk of tumorigenesis (represented in yellow). F) IL-17 signaling further upregulates the expression of STEAP4 in colon carcinoma cells. G) Continued inflammation, mediated by IL-17, continues to mobilize copper from the liver into systemic circulation, which further increases activation of ERK signaling, as the STEAP4-overexpressed cells take up additional copper from the blood, thus fueling a positive feedback cycle. H) After tumorigenesis, the established tumor causes dysregulation of normal colon homeostasis, thus sustaining a pro-inflammatory environment in the colon, paving the way for continued tumor growth and metastasis to potentially occur.

A crucial element in biology, copper is a required element in all living systems due to its ability to participate in one-electron transfer reactions. In humans, the ability of cells to take up copper from their extracellular requirement is dependent on a family of proteins known as the Six Transmembrane Epithelial Antigen of Prostate, or STEAP proteins. Additionally, it has previously been reported that copper is often elevated in malignant tissue samples compared to corresponding healthy tissue, including those found in colon cancer [75]. Previous data from the Li lab revealed that increased expression of STEAP4 is induced by stimulation with IL-17 [76]. Data from experiments presented in this thesis show that both overexpression of STEAP4, and stimulation with IL-17 increases the amount of copper taken up by colorectal cancer cells, the rate of which in the latter case agrees with data previously reported in human embryonic kidney cells [13]. Further data indicate that overexpression of STEAP4 in colon cancer cells enhances activation of the ERK pathway, which has previously been implicated in colorectal cancer [38], by IL-17 stimulation, suggesting that copper plays a critical role in this signaling process.

The most common site of distant colorectal cancer metastases is the liver. Upon the occurrence of colon cancer metastasis to the liver, the disease's prognosis becomes dismal [102]. Data presented here suggest that upon induction of intestinal inflammation, copper is mobilized from the liver into systemic circulation, which agrees with data previously reported indicating that this occurs in a mouse model of breast cancer as well [92]. Additionally, it was found that treatment with the copper chelator ammonium tetrathiomolybdate, used to treat copper overload in Wilson's Disease, potentially reduces the number of tumor nodules that develop in the colon in a model of inflammation-

associated colorectal cancer, though further investigation is required to provide convincing evidence of this conclusion. It is suggested that copper depletion therapy could slow the growth of colorectal tumors, and possibly reduce the instances of tumor metastases. Further study into this avenue of treatment is suggested.

The progress that has been made into describing the mechanisms of colon tumorigenesis and tumor progression, particularly in the context of an inflammatory microenvironment, has been encouraging. However, for people afflicted with the condition, it is still not enough. It is the author's hope that the experiments presented herein that detail the copper-dependent role of IL-17 in colorectal cancer cell growth will provide another step on the road to understanding, and ultimately curing, this devastating disease.

REFERENCES

1. McHenry, Charles, ed. (1992). The New Encyclopedia Britannica. 3 (15 ed.). Chicago: Encyclopedia Britannica, Inc. p. 612.
2. Festa, R. A., & Thiele, D. J. (2011). Copper: An essential metal in biology. Current Biol, 21(21), R877-R883.
3. Leary S.C., Winge D.R. The Janus face of copper: its expanding roles in biology and the pathophysiology of disease. Meeting on Copper and Related Metals in Biology. EMBO Rep. 2007; 8:224-227.
4. Karlin, K. D. (2013). Bioinorganic chemistry of copper.
5. Ohgami R., Campagna D., McDonald A., Fleming M. The Steap proteins are metalloreductases. Blood. 2006; 108(4):1388–1394.
6. Wyman S., Simpson R., McKie A., Sharp P. Dcytb (Cybrd1) functions as both a ferric and a cupric reductase in vitro. FEBS letters. 2008; 582:1901–6.
7. Prohaska, J., & Gybina, A. (2004). Intracellular copper transport in mammals. J Nutr, 134(5), 1003-1006.
8. Arredondo M., Nunez M. Iron and copper metabolism. Mol Aspects Med. 2005; 26: 313–327.
9. La Fountaine, S., & Mercer, J. (2007). Trafficking of the copper-ATPases, ATP7A and ATP7B: Role in copper homeostasis. Archives of Biochemistry and Biophysics, 463(2), 149-167.
10. Linder, M., et al. (1998). Copper transport. Am J Clin Nutr, 67(5), 965S-971S.
11. Bost M., Houdart S., Oberli M., Kalonji E., Huneau J., Margaritis I. Dietary copper and human health: current evidence and unresolved issues. J Trace Elem Med Biol. 2016; 35: 107–15.
12. Olivares, M., et al. (2008). Present situation of biomarkers for copper status. Am J Clin Nutr, 88(3), 859S-862S.
13. Ohgami, R., et al. (2006). The Steap proteins are metalloreductases. Blood, 108(4), 1388-1394.

14. Large Intestine - National Library Of Medicine - Pubmed Health - https://www.ncbi.nlm.nih.gov/pubmedhealth/PMHT0022246/
15. Quigley, E. (2013). Gut Bacteria in Health and Disease. Gastroenterol and Hepatol, 9(9), 560-569.
16. Worldwide Data - https://www.wcrf.org/int/cancer-facts-figures/worldwide-data
17. What is Colon Cancer: Statistics - http://www.ccalliance.org/get-information/what-is-colon-cancer/statistics/
18. Colorectal Cancer Risk Factors - http://www.cancer.org/cancer/colon-rectal-cancer/causes-risks-prevention/risk-factors.html
19. Haggar, F., Boushey, R. Colorectal Cancer Epidemiology: Incidence, Mortality, Survival, and Risk Factors. Clinics in Colon and Rectal Surgery. 2009; 22(4):191-197.
20. Colorectal Cancer Facts & Figures 2017 – 2019. Retrieved from https://www.cancer.org/content/dam/cancer-org/research/cancer-facts-and-statistics/colorectal-cancer-facts-and-figures/colorectal-cancer-facts-and-figures-2017-2019.pdf
21. Cancer Stat Facts: Colorectal Cancer - https://seer.cancer.gov/statfacts/html/colorect.html
22. Siegel, R., et al. (2017). Colorectal Cancer Incidence Patterns in the United States, 1974–2013. JNCI, 109(8).
23. Colorectal Cancer - http://www.cancer.org/cancer/colonandrectumcancer/detailedguide/colorectal-cancer-key-statistics
24. Breen, N., et al. (2017). Assessing disparities in colorectal cancer mortality by socioeconomic status using new tools: Health disparities calculator and socioeconomic quintiles. Cancer Causes Control, 28(2), 117-125.
25. Kunzmann, A. (2015). Dietary fiber intake and risk of colorectal cancer and incident and recurrent adenoma in the Prostate, Lung, Colorectal, and Ovarian Cancer Screening Trial. Am J Clin Nutr, 102(4), 881-890.
26. Gram, I., et al. (2009). Cigarette smoking and risk of colorectal cancer among Norwegian women. Cancer Causes Control, 20(6), 895-903.

27. Botteri, E., et al. (2008). Cigarette smoking and adenomatous polyps: A meta-analysis. Gastroenterol, 134(2), 388-395.
28. Slattery, M. (2004). Physical activity and colorectal cancer. Sports Med, 34(4), 239-252.
29. Boffetto, P., & Hashibe, M. (2006). Alcohol and cancer. Oncology, 7(2), 149-156.
30. Valderrama-Treviño, A. (2017). Hepatic Metastasis from Colorectal Cancer. Euroasian J Hepatogastroenterol, 7(2), 166-175.
31. Manfredi S, Lepage C, Hatem C, et al. Epidemiology and management of liver metastases from colorectal cancer. Ann Surg. 2006; 244(2):254–9.
32. Terzic, J., et al. Inflammation and colon cancer. Gastroenterol. 2010; 138(6), 2101-2114.
33. Bollrath J., Greten F. IKK/NF-kappaB and STAT3 pathways: central signalling hubs in inflammation-mediated tumour promotion and metastasis. EMBO Rep. 2009; 10: 1314–1319.
34. Hata, K. (2002). IL-17 stimulates inflammatory responses via NF-kappaB and MAP kinase pathways in human colonic myofibroblasts. Am J Physiol Gastrointest Liver Physiol, 282(6), 1035-1044.
35. Perkins ND. Integrating cell-signalling pathways with NF-kappaB and IKK function. Nat Rev Mol Cell Biol. 2007; 8(1):49–62.
36. Jaramillo M., Zhang D. The emerging role of the Nrf2-Keap1 signaling pathway in cancer. Genes Dev. 2013; 27(20):2179–2191.
37. Zhang, W., & Liu, H. (2002). MAPK signal pathways in the regulation of cell proliferation in mammalian cells. Cell Research, 12(1), 9-18.
38. Kim, E., & Choi, E. (2010). Pathological roles of MAPK signaling pathways in human diseases. Biochim Biophys Acta, 1802(4), 396-405.
39. H. Nagahara., et al. (2005). Somatic mutations of epidermal growth factor receptor in colorectal carcinoma, Clin. Cancer Res. 11(4) 1368–1371.
40. Chemistry LibreTexts - Chelation - http://chem.libretexts.org/Core/Inorganic_Chemistry/Coordination_Chemistry/Complex_Ion_Equilibria/Chelation

41. Hedera, P. (2017). Update on the clinical management of Wilson's disease. Appl Clin Genet, 13(10), 9-19.
42. Denoyer, D. et al. Targeting copper in cancer therapy: 'Copper That Cancer', Metallomics. 2015; 7:1459-1476.
43. Ferrero-Miliani L., Nielsen O., Andersen P., Girardin S. Chronic inflammation: importance of NOD2 and NALP3 in interleukin-1beta generation. Clin Exp Immunol. 2007; 147(2):227–35.
44. Ahmed, A. (2011). An overview of inflammation: Mechanism and consequences. Frontiers in Biol, 6(274).
45. Gaffen S. An overview of IL-17 function and signaling. Cytokine. 2008; 43:402–407.
46. Wang L., Yi T., Kortylewski M., Pardoll D., Zeng D., Yu H. IL-17 can promote tumor growth through an IL-6-Stat3 signaling pathway. J Exp Med. 2009, 206(7):1457–1464.
47. Kryczek I, et al. Endogenous IL-17 contributes to reduced tumor growth and metastasis. Blood. 2009; 114:357–359.
48. Rouvier, E., et al. (1993). CTLA-8, cloned from an activated T cell, bearing AU-rich messenger RNA instability sequences, and homologous to a herpesvirus saimiri gene. J Immunol, 150(12), 5445-5456.
49. Kolls, J., Lindén, A. (2004). Interleukin-17 Family Members and Inflammation. Immunity, 21(4), 467-476.
50. Gaffen, S. (2009). Structure and signalling in the IL-17 receptor family. Nat Rev Immunol, 9, 556-567.
51. Yao, Z., et al. (1995). Herpesvirus saimiri encodes a new cytokine, IL-17, which binds to novel cytokine receptor. Immunity, 3, 811-821.
52. McGeachy, M., et al. (2007). TGF-β and IL-6 drive the production of IL-17 and IL-10 by T cells and restrain TH-17 cell–mediated pathology. Nat Immunol, 8, 1390-1397.
53. Santana, M., Esquivel-Guadarrama, F. (2006). Cell biology of T cell activation and differentiation. Int Rev Cytol, 250, 217-274.

54. Liang, S., et al. (2006). Interleukin (IL)-22 and IL-17 are coexpressed by Th17 cells and cooperatively enhance expression of antimicrobial peptides. J Exp Med, 203(10), 2271-2279.
55. Pappu, R., Rutz, S., & Ouyang, W. (2012). Regulation of epithelial immunity by IL-17 family cytokines. Trends in Immunol, 33(7), 343–349.
56. Nguyen, L., Haney, E., Vogel, H. (2011). The expanding scope of antimicrobial peptide structures and their modes of action. Trends in Biotech, 29(9), 464-472.
57. Korn, T., et al. (2009). IL-17 and Th17 cells. Annu Rev Immunol. 27, 485-517.
58. Fujino, S., et al. (2003). Increased expression of interleukin 17 in inflammatory bowel disease. Gut, 52(1), 65-70.
59. Tabarkiewicz, J., et al. (2015). The Role of IL-17 and Th17 Lymphocytes in Autoimmune Diseases. Arch Immunol Ther Exp, 63, 435-449.
60. Hohenberger, M., et al. (2017). Interleukin-17 Inhibition: Role in Psoriasis and Inflammatory Bowel Disease. J Dermatolog Treat.
61. Taketo M., Edelmann W. Mouse models of colon cancer. Gastroenterology. 2009; 136:780–98.
62. Wirtz S., Neufert C., Weigmann B., Neurath M. Chemically induced mouse models of intestinal inflammation. Nat Protoc. 2007; 2:541–546.
63. McIntyre, R. et al. Mouse models of colorectal cancer as preclinical models. BioEssays. 2015; 37(8): 909-920.
64. The Nobel Prize - The Nobel Prize in Physiology or Medicine 1954 - https://www.nobelprize.org/prizes/medicine/1954/summary/
65. Eberwine, J., Kim, T. (2010). Mammalian cell transfection: the present and the future. Anal Bioanal Chem, 397(8), 3173–3178.
66. Life Science Articles - Editorial Articles - Stable vs. Transient Transfection of Eukaryotic Cells - https://www.biocompare.com/Editorial-Articles/126324-Transfection/
67. Kimple, M., Brill, A., Pasker, R. (2013). Overview of Affinity Tags for Protein Purification. Curr Protoc Protein Sci, 73.
68. Allen, N., Plagge, A., Kelsey, G. (2000). Directed Mutagenesis in Embryonic Stem Cells. Mouse Genet and Transgenics, 259–263.

69. Gomez-Martinez, M., Schmitz, D., Hergovich, A. (2013). Generation of Stable Human Cell Lines with Tetracycline-inducible (Tet-on) shRNA or cDNA Expression. J Vis Exp, 73.

70. Chemistry LibreTexts - Atomic Absorption Spectroscopy - https://chem.libretexts.org/Textbook_Maps/Analytical_Chemistry/Book%3A_Analytical_Chemistry_2.0_(Harvey)/10_Spectroscopic_Methods/10.4%3A_Atomic_Absorption_Spectroscopy

71. Chassaing, B., et al. (2014). Dextran Sulfate Sodium (DSS)-Induced Colitis in Mice. Curr Protoc Immunol, 104(15), 1-14.

72. Walling, C., Kato, S. (1971). Oxidation of alcohols by Fenton's reagent. Effect of copper ion. J Am Chem Soc, 93(17), 4275-4281.

73. Forman, H., Torres, M. (2002). Reactive Oxygen Species and Cell Signaling: Respiratory Burst in Macrophage Signaling. Am J Respir Crit Care Med, 166(12), S4-S8.

74. Xie, H., Kang, Y. (2009). Role of copper in angiogenesis and its medicinal implications. Curr Med Chem, 16(10), 1304-1314.

75. Margalioth, E., Schenker, J., Chevion, M. (1983). Copper and Zinc levels in normal and malignant tissues. Cancer, 52(5), 868-872.

76. Wu, L., et al. (2015). A novel IL-17 signaling pathway controlling keratinocyte proliferation and tumorigenesis via the TRAF4–ERK5 axis. J Exp Med, 212(10), 1571-1587.

77. Milanino, R., et al. (1993). Copper and zinc body levels in inflammation: An overview of the data obtained from animal and human studies. Agents Actions, 39(3), 195-209.

78. Wang, K. (2017). Targeting IL-17 for cancer-associated inflammation and immunity. J Immunol, 198(1).

79. Chae, W., et al. (2010). Ablation of IL-17A abrogates progression of spontaneous intestinal tumorigenesis. Proc Natl Acad Sci, 107(12), 5540-5544.

80. Wu, D., et al. (2013). Interleukin-17: a promoter in colorectal cancer progression. Clin Dev Immunol, 2013, Article ID 436307, 7 pages.

81. Cua, D., Tato, C. (2010). Innate IL-17-producing cells: the sentinels of the immune system. Nat Rev Immunol, 10(7), 479-489.
82. N. Takahashi, I., et al. (2008). IL-17 produced by Paneth cells drives TNF-induced shock. J Exp Med, 205(8), 1755–1761.
83. Kaplan, J., Lutsenko, S. (2009). Copper Transport in Mammalian Cells: Special Care for a Metal with Special Needs. J Biol Chem, 284(38), 25461–25465.
84. Zamble, D., Lippard, S. (1995). Cisplatin and DNA repair in cancer chemotherapy. Trends Biochem Sci, 20(10), 435-439.
85. Dasari, S., Tchounwou, P. (2014). Cisplatin in cancer therapy: molecular mechanisms of action. Eur J Pharmacol, 740, 364-378.
86. Kilari, D., Guancial, E., Kim, E. (2016). Role of copper transporters in platinum resistance. World J Clin Oncol, 7(1), 106-113.
87. Ishida S, McCormick F, Smith-McCune K, Hanahan D. (2010). Enhancing tumor-specific uptake of the anticancer drug cisplatin with a copper chelator. Cancer Cell, 17(6), 574–583.
88. Palumaa, P., et al. (2004). Metal-binding mechanism of Cox17, a copper chaperone for cytochrome c oxidase. (382) Pt. 1, 307-314.
89. Larin, D., et al. (1999). Characterization of the interaction between the Wilson and Menkes disease proteins and the cytoplasmic copper chaperone, HAH1p. J Biol Chem, 274(40), 28497-28504.
90. Casareno, L., Waggoner, D., Gitlin, J. (1998). The copper chaperone CCS directly interacts with copper/zinc superoxide dismutase. J Biol Chem, 273(37), 23625-23628.
91. Collins, J., Prohaska, J., Knutson, M. (2010). Metabolic crossroads of iron and copper. Nutr Rev, 68(3), 133-147.
92. Majumder, S., Dutta, P., Choudhuri, S. (2005). The Role of Copper in Development of Drug Resistance in Murine Carcinoma. 1(6), 563-573.
93. Calvert, P., Frucht, H. (2002). The genetics of colorectal cancer. Ann Intern Med, 137(7), 603-612.
94. Fang, J., Richardson, B. (2005). The MAPK signalling pathways and colorectal cancer. Lancet Oncol, 6(5), 322-327.

95. McCubrey, J., et al. (2007). Roles of the Raf/MEK/ERK pathway in cell growth, malignant transformation and drug resistance. Biochim Biophys Acta, 1773(8), 1263-1284.

96. Treisman, R. (1994). Ternary complex factors: growth factor regulated transcriptional activators. Curr Opin Genet Dev, 4(1), 96-101.

97. Chen, Y., et al. (2011). IL-17A stimulates the production of inflammatory mediators via Erk1/2, p38 MAPK, PI3K/Akt, and NF-kappaB pathways in ARPE-19 cells. Mol Vis, 17, 3072–3077.

98. Turski, M., et al. (2012). A Novel Role for Copper in Ras/Mitogen-Activated Protein Kinase Signaling. Mol Cell Biol, 32(7), 1284-1295.

99. Aggarwal, A., Bhatt, M. (2018). Advances in Treatment of Wilson's Disease. Tremor Other Hyperkinet Mov, 8(525).

100. Zhou, W., et al. (2018). Tetrathiomolybdate Treatment Leads to the Suppression of Inflammatory Responses through the TRAF6/NFκB Pathway in LPS-Stimulated BV-2 Microglia. Front Aging Neurosci, 10(9).

101. Sahota, S., et al. (2017). A phase II study of copper-depletion using tetrathiomolybdate (TM) in patients (pts) with breast cancer (BC) at high risk for recurrence: Updated results. J Clin Oncol, 35(15S).

102. American Cancer Society - Survival Rates for Colorectal Cancer, by Stage - https://www.cancer.org/cancer/colon-rectal-cancer/detection-diagnosis-staging/survival-rates.html

103. Brewer, G. (2005). Copper lowering therapy with tetrathiomolybdate as an antiangiogenic strategy in cancer. Curr Cancer Drug Targets, 5(3), 195-202.

104. American Cancer Society - American Cancer Society Guideline for Colorectal Cancer Screening - https://www.cdc.gov/media/releases/2013/p1105-colorectal-cancer-screening.html

APPENDIX

Figure 1.1 – Copper homeostasis in mammalian cells

This Agreement between Cleveland State University -- Evan Martin ("You") and Royal Society of Chemistry ("Royal Society of Chemistry") consists of your license details and the terms and conditions provided by Royal Society of Chemistry and Copyright Clearance Center.

License Number
4394880977696

License date
Jul 23, 2018
Licensed Content Publisher
Royal Society of Chemistry

Licensed Content Publication
Metallomics

Licensed Content Title
Targeting copper in cancer therapy: 'Copper That Cancer'

Licensed Content Author
Delphine Denoyer,Shashank Masaldan,Sharon La Fontaine,Michael A. Cater

Licensed Content Date
Aug 21, 2015

Licensed Content Volume
7

Licensed Content Issue
11

Type of Use
Thesis/Dissertation

Requestor type
academic/educational

Portion
figures/tables/images

Number of figures/tables/images
1

Format
print and electronic

Distribution quantity
1

Will you be translating?
No

Title of the thesis/dissertation
IL-17 DRIVES COPPER UPTAKE AND ACTIVATION OF GROWTH PATHWAYS IN

COLORECTAL CANCER CELLS IN A STEAP4-DEPENDENT MANNER

Expected completion date
Aug 2018

Estimated size
50

Requestor Location
Cleveland State University
United States
Attn: Cleveland State University

Billing Type
Invoice

Total
0.00 USD

Figure 1.2 – Human copper metabolism

This Agreement between Cleveland State University -- Evan Martin ("You") and Oxford University Press ("Oxford University Press") consists of your license details and the terms and conditions provided by Oxford University Press and Copyright Clearance Center.

License Number	4394890563723
License date	Jul 23, 2018
Licensed Content Publisher	Oxford University Press
Licensed Content Publication	Nutrition Reviews
Licensed Content Title	New developments in the regulation of intestinal copper absorption
Licensed Content Author	van den Berghe, Peter VE; Klomp, Leo WJ
Licensed Content Date	Nov 1, 2009
Licensed Content Volume	67
Licensed Content Issue	11
Type of Use	Thesis/Dissertation
Requestor type	Educational Institution/Non-commercial/ Not for-profit
Format	Print and electronic
Portion	Figure/table
Number of figures/tables	1
Will you be translating?	No
Title	IL-17 DRIVES COPPER UPTAKE AND ACTIVATION OF GROWTH PATHWAYS IN COLORECTAL CANCER CELLS IN A STEAP4-DEPENDENT

	MANNER
Instructor name	n/a
Institution name	n/a
Expected presentation date	Aug 2018
Portions	Figure 1
Requestor Location	Cleveland State University United States
Publisher Tax ID	GB125506730
Billing Type	Invoice
Total	0.00 USD

Figure 1.3 – A schematic description of STEAP4's protein structure and molecular functions

Request to reproduce figures or tables in other publications or journals: There is no need to obtain permission if copyrights of the figures or tables belong to Ivyspring International Publisher. Please acknowledge the original source of publication in our journal with full citation. If the copyrights of the figures or tables belong to other publishers or authors, please contact the original publishers or authors for permissions.

(Obtained from: http://www.ijbs.com/ms/terms)

Yoo, S., Cheong, J., & Kim, H. (2014). STAMPing into Mitochondria. Int J Biol Sci, 10(3), 321-326. https://www.ncbi.nlm.nih.gov/pmc/articles/PMC3957087/

Figure 1.4 – Stages of colorectal cancer

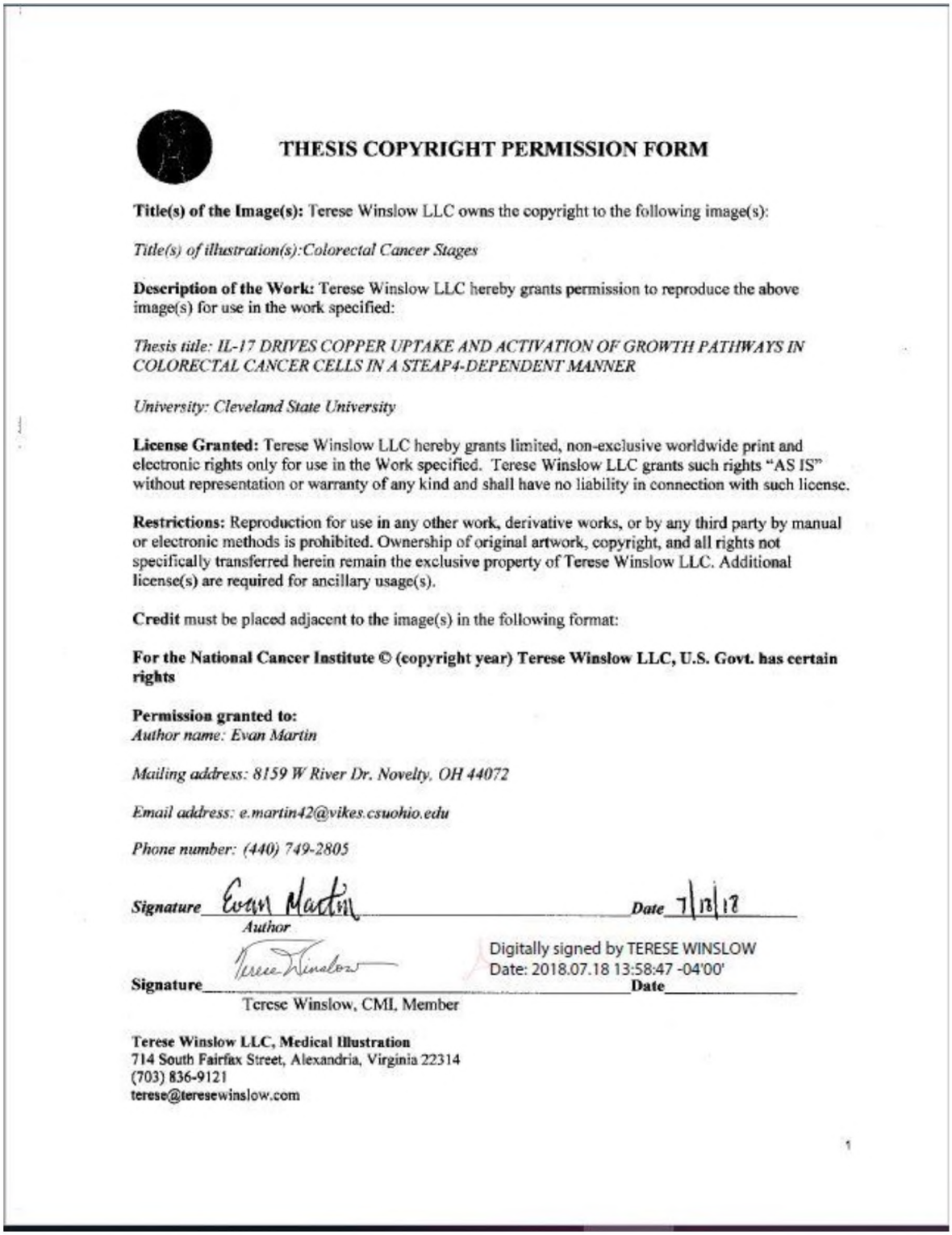

THESIS COPYRIGHT PERMISSION FORM

Title(s) of the Image(s): Terese Winslow LLC owns the copyright to the following image(s):

Title(s) of illustration(s):Colorectal Cancer Stages

Description of the Work: Terese Winslow LLC hereby grants permission to reproduce the above image(s) for use in the work specified:

Thesis title: IL-17 DRIVES COPPER UPTAKE AND ACTIVATION OF GROWTH PATHWAYS IN COLORECTAL CANCER CELLS IN A STEAP4-DEPENDENT MANNER

University: Cleveland State University

License Granted: Terese Winslow LLC hereby grants limited, non-exclusive worldwide print and electronic rights only for use in the Work specified. Terese Winslow LLC grants such rights "AS IS" without representation or warranty of any kind and shall have no liability in connection with such license.

Restrictions: Reproduction for use in any other work, derivative works, or by any third party by manual or electronic methods is prohibited. Ownership of original artwork, copyright, and all rights not specifically transferred herein remain the exclusive property of Terese Winslow LLC. Additional license(s) are required for ancillary usage(s).

Credit must be placed adjacent to the image(s) in the following format:

For the National Cancer Institute © (copyright year) Terese Winslow LLC, U.S. Govt. has certain rights

Permission granted to:
Author name: Evan Martin

Mailing address: 8159 W River Dr. Novelty, OH 44072

Email address: e.martin42@vikes.csuohio.edu

Phone number: (440) 749-2805

Signature Evan Martin ***Date*** 7/18/18
Author

Signature Terese Winslow Digitally signed by TERESE WINSLOW Date: 2018.07.18 13:58:47 -04'00' **Date**
Terese Winslow, CMI, Member

Terese Winslow LLC, Medical Illustration
714 South Fairfax Street, Alexandria, Virginia 22314
(703) 836-9121
terese@teresewinslow.com

1

Figure 1.5 – MAPK/ERK signaling in the pathogenesis of cancer

This Agreement between Cleveland State University -- Evan Martin ("You") and

Elsevier ("Elsevier") consists of your license details and the terms and conditions provided by Elsevier and Copyright Clearance Center.

License Number	4394881286070
License date	Jul 23, 2018
Licensed Content Publisher	Elsevier
Licensed Content Publication	The Lancet Oncology
Licensed Content Title	The MAPK signalling pathways and colorectal cancer
Licensed Content Author	Jing Yuan Fang,Bruce C Richardson
Licensed Content Date	May 1, 2005
Licensed Content Volume	6
Licensed Content Issue	5
Licensed Content Pages	6
Type of Use	reuse in a thesis/dissertation
Portion	figures/tables/illustrations
Number of figures/tables/illustrations	1
Format	both print and electronic
Are you the author of this Elsevier article?	No
Will you be translating?	No
Original figure numbers	MAPK signalling in pathogenesis
Title of your thesis/dissertation	IL-17 DRIVES COPPER UPTAKE AND ACTIVATION OF GROWTH PATHWAYS IN COLORECTAL CANCER CELLS IN A STEAP4-DEPENDENT MANNER
Expected completion date	Aμg 2018
Estimated size (number of pages)	50
Requestor Location	Cleveland State University United States
Publisher Tax ID	98-0397604
Total	0.00 USD

Figure 1.6 – Immune system signaling and inflammation play a critical role in the risk of tumorigenesis and cancer progression.

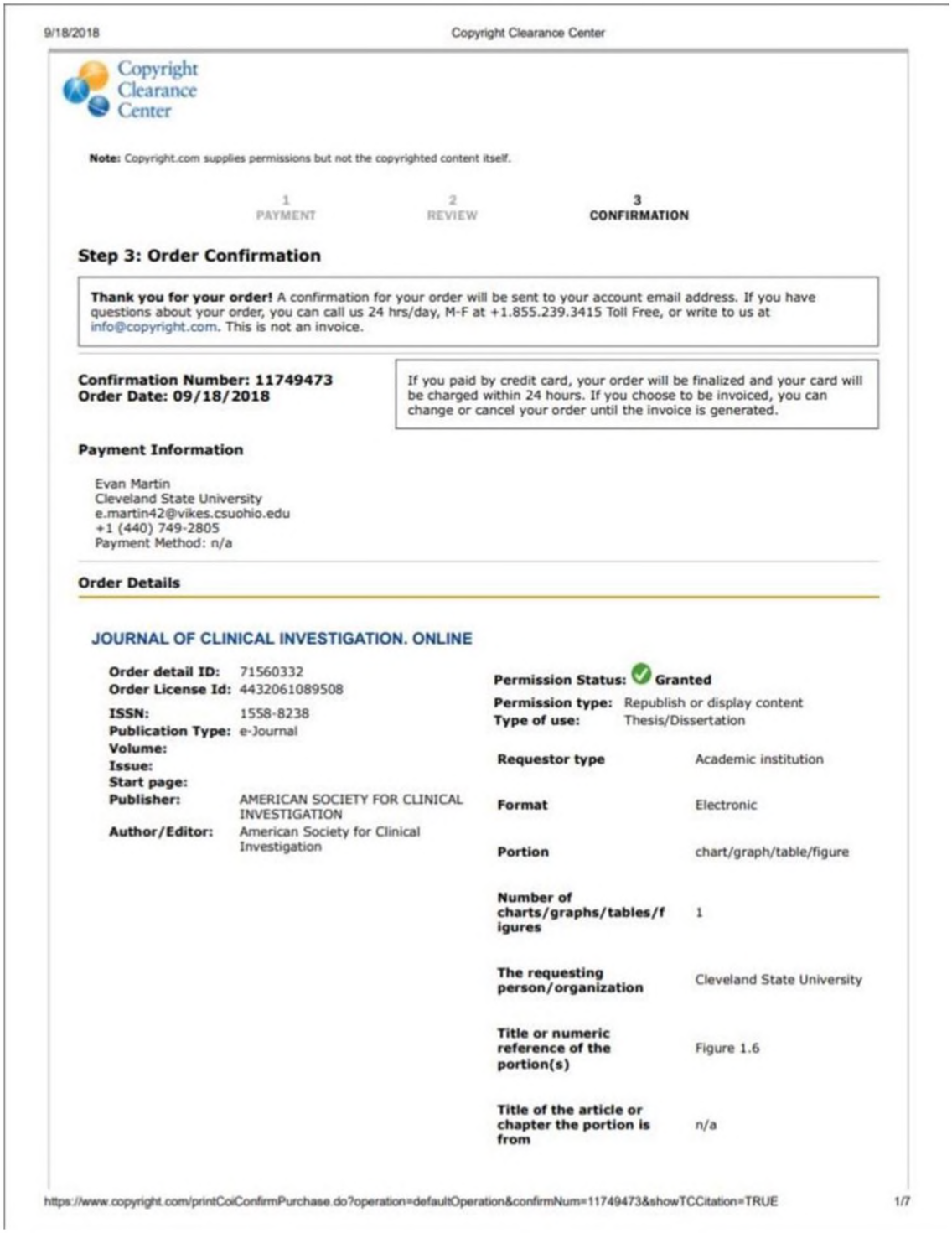

Figure 1.7 – IL-17 increases expression of many genes through activation of various downstream signaling pathways.

Rights and Permissions

Non-commercial requests

Authors may reproduce an article, in whole or in part, in a thesis or dissertation at no cost providing the original source is attributed.

(Obtained from: http://www.portlandpresspublishing.com/content/rights-and-permissions)

Zhu, S., Qian, Y. (2012). IL-17/IL-17 receptor system in autoimmune disease: mechanisms and therapeutic potential. Clin Sci, 122(11), 487-511.

Figure 1.8 – IL-17 and the pathogenesis of cancer

This is an open access article distributed under the Creative Commons Attribution License, which permits unrestricted use, distribution, and reproduction in any medium, provided the original work is properly cited.

(Obtained from: https://www.ncbi.nlm.nih.gov/pmc/articles/PMC3870650/)

Wu, D. (2013). Interleukin-17: A promoter in colorectal cancer progression. Clin Dev Immunol. https://www.ncbi.nlm.nih.gov/pmc/articles/PMC3870650/

Figure 1.9 – Molecular structure of dextran sodium sulfate (DSS) and azoxymethane (AOM).

DSS:

Permission Requests

For the vast majority of articles in Hindawi journals, you do not need to seek permission from Hindawi for reuse. The copyright of most articles remains with the authors, who have chosen to make the articles available for reuse under an open license, such as the Creative Commons Attribution License (CC-BY). These licenses permit reuse and adaptation, as long as the original authors are cited. The applicable license for all articles is included in the front matter of the article in human- and machine-readable formats.

Rarely, Hindawi journals will contain material republished with permission under a more restrictive license. Where applicable, this will be clearly marked. In these cases, you may need to seek permission for reuse from the copyright holder.

(Obtained from: https://www.hindawi.com/copyright/)

Tanaka, T. (2011). Development of an Inflammation-Associated Colorectal Cancer Model and Its Application for Research on Carcinogenesis and Chemoprevention. Int J Inflam, 2012.

AOM:

Commons:Reusing content outside Wikimedia

The Wikimedia Foundation owns almost none of the content on Wikimedia sites — the content is owned, instead, by the individual creators of it. However, almost all content hosted on Wikimedia Commons may be freely reused subject to certain restrictions (in many cases). You do not need to obtain a specific statement of permission from the licensor(s) of the content unless you wish to use the work under different terms than the license states.

(Obtained from:
https://commons.wikimedia.org/wiki/Commons:Reusing_content_outside_Wikimedia)

Image obtained from:
https://en.wikipedia.org/wiki/Azoxymethane#/media/File:Azoxymethane.png

Figure 2.2 – Overview of an atomic absorption spectrophotometer

Sent by: Evan Martin <e.martin42@vikes.csuohio.edu>

Sent on: Tue, Jul 17, 2018 at 3:12 PM

Sent to: labtraining@lab-training.com

Subject: Atomic absorption diagram

Hello,

My name is Evan Martin, and I am a master's candidate in the Department of Chemistry at Cleveland State University. I am currently writing a thesis on the role of copper metabolism in colorectal cancer, and I came across a diagram on your website (http://lab-training.com/aas/) titled "Double Beam AAS Schematic Diagram".

I would like to request permission to include this diagram in my thesis. If you have any questions about my project, please contact me at e.martin42@vikes.csuohio.edu and I would be happy to answer them. Thank you for your consideration, and I hope to hear from you soon.

Regards,
Evan

Sent by: Dr. Saurabh Arora <saurabharora@arbropharma.com>

Sent on: Wed, JμL 18, 2018 at 12:30 AM

Sent to: e.martin42@vikes.csuohio.edu

Subject: Re: Atomic absorption diagram

Dear Evan

Please feel free to use the diagram.
